



UNIVERSITEIT VAN PRETORIA  
UNIVERSITY OF PRETORIA  
YUNIBESITHI YA PRETORIA

# Characterization of medium temperature gasifier pitch

By

Gedion John Papole

Submitted in partial fulfilment of the requirements for the degree

Master of Science

Department of Chemistry  
Faculty of Natural and Agricultural Sciences  
University of Pretoria  
Pretoria

April 2012

## DECLARATION

I, Gedion John Papole, declare that the dissertation I hereby submit for the degree Master of Science in Chemistry is my own work. I have not previously submitted it for degree purposes at any other university.

SIGNED ON THIS.....DAY OF APRIL 2012

**Gedion John Papole (Student)**

**Prof. Walter Focke (Supervisor)**

.....

.....

## ABSTRACT

Pitches are important precursors for carbon materials. They are usually obtained by thermal treatment of petroleum and coal fractions. Pitches have higher carbon content and are capable of developing into graphitisable carbons upon heat treatment. Petroleum pitches are generally less aromatic than coal tar pitches.

Medium-temperature gasifier pitch (MTP), from Sasol's Lurgi process, is a potential precursor for graphitisable carbon. MTP showed a high degree of solubility in several organic solvents, namely dimethylformamide, quinoline, tetrahydrofuran, pyridine, morpholine, benzene, toluene, xylene and acetone. It was virtually insoluble in *n*-hexane, cyclohexane, cyclohexanol, acetonitrile and formamide. MTP pitch was partially soluble in methanol and had a solubility limit of 40 g/l at ambient temperature.

MTP samples were spiked with boron to make 1000 ppm B-containing samples. The boron distribution coefficient was defined as the ratio of the boron contents of the insoluble pitch residue to the methanol-soluble pitch extracts, using a mass balance. This justified the decision to define the apparent boron partition coefficients based on the boron content of the recovered pitch residues. 4-(dibenzofuranyl) boronic acid (DBA), 2-phenoxyphenyl boronic acid (PBA), *p*-tolylboronic acid (TBA) and phenylboronic acid (PLA) were retained the most in the residues after methanol extraction. Over 500 ppm of PBA, TBA and PLA were retained in the pitch residues following methanol extraction.

The results showed that methanol extracted substituted boron acid model compounds. Methanol dissolved mostly low molecular mass/aliphatic species, which are not important for graphitisation.

The thermomechanical analysis (TMA) results showed that MTP has a low softening point compared with the methanol-insoluble (MI) fractions. The attenuated total reflectance (ATR) results showed that the benzene-insoluble (BI), toluene-insoluble (TI) and MI fractions had more intense aromatic C–H stretching peaks than their corresponding soluble fractions. Elemental analysis and the solid-state <sup>13</sup>C nuclear magnetic resonance (NMR) results revealed that the benzene-, toluene- and methanol-insoluble fractions are more aromatic than their corresponding soluble fractions. The

order of the aromaticity index for the insoluble fractions was as follows:  
MTP<MI<TI<BI.

Matrix-assisted laser desorption (MALDI) analysis of the mass distribution revealed that the majority of compounds in MTP and its soluble and insoluble fractions were in the low molecular mass range, i.e. 190–388 atomic mass units. The thermal analysis results showed that the benzene-, toluene- and methanol-insoluble fractions were thermally stable and had higher carbon yields than their corresponding soluble fractions. MTP was thermally more stable than the methanol-, toluene- and benzene-soluble fractions.

Evaluation of the polycyclic aromatic hydrocarbons (PAHs) by gas chromatography-mass spectrometry (GC-MS) showed that the methanol-insoluble fractions had lower PAH contents than MTP and MI.

## ACKNOWLEDGEMENTS

I am deeply indebted to the following people, who in one way or the other contributed so much in the success of this work:

- My promoter Prof. Walter Focke for his supervision and overwhelming support, particularly those one-to-one sessions I have had with him.
- Prof. Brian Rand for his invaluable contribution towards the success of this work and most importantly for his patience.
- Prof. Ncholu Manyala for his academic advice and words of encouragement when gloom deepened during this study.
- The contribution by all the Carbon Group students is much appreciated, most importantly their inputs and criticism, which helped me to compile this work.
- Sasol for provision of samples, and the Chemistry Departments at the University of Pretoria and the University of Stellenbosch for analysis of samples.
- The Carbon Chair under the South African Research Chair Initiative (SARChI) for affording me the opportunity to attend an international conference on Carbon held at Clemson University in South Carolina, United States.
- This work could not have been a success without the financial support I received from SANHARP. A million thanks to the SANHARP Team. Please continue with the good work that you are doing.
- Suzette your support has been phenomenal throughout this work and I am grateful for that. I could not have performed some of the experiments without the assistance of Rainer Schumacher; thank you Mr Schumacher.
- The unwavering support from my family and friends and for their understanding when I was not there when they needed me.
- Above all, I would like to express my sincere gratitude to the governor of the universe, the omnipotent God who gave me the strength and kept me going.

## TABLE OF CONTENTS

<b>ABSTRACT.....</b>	<b>I</b>
<b>ACKNOWLEDGEMENTS .....</b>	<b>III</b>
<b>LIST OF FIGURES .....</b>	<b>VII</b>
<b>LIST OF TABLES .....</b>	<b>X</b>
<b>LIST OF ABBREVIATIONS .....</b>	<b>XI</b>
<b>CHAPTER ONE: INTRODUCTION .....</b>	<b>1</b>
1.1 Background.....	1
1.2 Aims and Objectives .....	2
<b>CHAPTER TWO: LITERATURE REVIEW .....</b>	<b>4</b>
2.1 Pitch .....	4
2.2 Coal Tar Pitches .....	5
2.3 Petroleum Pitches.....	6
2.4 Characterisation of Pitch.....	6
2.4.1 Solubility.....	7
2.4.2 Solvent fractionation.....	8
2.4.3 Nuclear magnetic resonance .....	10
2.4.4 Infrared spectroscopy.....	12
2.5 Thermal Treatment of Pitches.....	13
2.5.1 Mesophase.....	13
2.5.2 Carbonisation .....	17
2.5.3 Graphitisation.....	19
2.6 Effect of Boron on Graphitisation.....	22
2.7 Boron Removal Methods .....	23
2.8 Boron Determination Methods .....	24
2.8.1 Curcumin.....	24
2.8.2 Carminic acid .....	27

2.8.3	Quinalizarin.....	27
2.8.4	1,1'-dianthrimide .....	28
2.8.5	Methylene blue-tetrafluoroborate .....	28
2.9	Boron Uses.....	29
<b>CHAPTER THREE: EXPERIMENTAL .....</b>		<b>32</b>
3.1	Materials .....	32
3.2	Ash Determination .....	32
3.3	Solubility Experiments.....	32
3.4	Extract Recovery.....	33
3.5	Doping of Boron Model Compounds .....	34
3.5.1	Simulated boron removal.....	35
3.5.2	Boron determination .....	37
3.6	Structural Analysis.....	37
3.6.1	Elemental analysis .....	37
3.6.2	Infrared spectroscopy.....	37
3.6.3	Nuclear magnetic resonance .....	38
3.6.4	MALDI-TOF.....	38
3.6.5	GC-MS.....	39
3.7	Thermal Analysis.....	40
3.7.1	Softening point.....	40
3.7.2	Thermogravimetric analysis.....	40
3.7.3	Differential thermogravimetry .....	41
<b>CHAPTER FOUR: RESULTS AND DISCUSSION .....</b>		<b>42</b>
4.1	Solubility.....	42
4.2	Determination of Boron .....	45
4.3	Structural Analysis.....	46
4.3.1	Elemental analysis .....	46
4.3.2	ATR-infrared spectroscopy.....	47
4.3.3	Nuclear magnetic resonance .....	51
4.3.4	Molecular mass distributions .....	56

4.3.5	Evaluation of PAHs by GC-MS.....	62
4.4	Thermomechanical Analysis.....	64
4.5	Thermogravimetric Analysis .....	66
<b>CHAPTER FIVE: CONCLUSIONS .....</b>		<b>71</b>
<b>CHAPTER SIX: REFERENCES .....</b>		<b>73</b>



## LIST OF FIGURES

Figure 2.1: Spider Wedge model of mesophase constituent molecules (Mochida et al., 2000).....	14
Figure 2.2: Typical mesogen units in different mesophase pitches (Mochida et al., 2000).....	15
Figure 2.3: Relationships between rodic and discotic shapes of mesogens in terms of temperature of formation of mesophase (Marsh et al., 1999) .....	16
Figure 2.4: A carbonisation model of acenaphthylene showing molecular size enlargement of aromatic systems (Mochida et al., 2001).....	19
Figure 2.5: Models for different structures of carbons proposed by Franklin (1951); (a) non-graphitising, (b) partially graphitising and (c) graphitising carbons....	20
Figure 2.6: Hexagonal unit of structure of graphite showing the $d_{002}$ -spacing (Kirk-Othmer, 2005).....	21
Figure 2.7: Structural forms of curcumin: (a) keto and (b) enol isomers. Curcumin is a chemical compound that can be used for quantifying boron (Iwunze, 2004) .....	25
Figure 2.8: Structure of rosocyanine, a curcumin-boron complex (Uppström, 1968). Curcumin reacts with boric acid to give a red complex, rosocyanine.....	26
Figure 2.9: Structure of rubrocurcumin. One curcumin molecule is replaced with an oxalate in rosocyanine to form rubrocurcumin (Uppström, 1968).....	26
Figure 3.1: Schematic diagram of a typical rotary evaporator for extract and solvent recovery (Pasto and Johnson, 1989) .....	34
Figure 3.2: Boron model compounds used for doping medium-temperature gasifier pitch (MTP). MTP was spiked with each model compound to prepare 0.1 wt % (1000 ppm) B samples .....	36

Figure 4.1: Solubility test results showing some powerful solvents for MTP. Experiments were conducted at ambient temperature with 1 g MTP in 10 ml of solvent for 2 days. ....	42
Figure 4.2: Solubility tests showing some good and poor solvents for MTP. Experiments were conducted at ambient temperature with 1 g of MTP in 10 ml of solvent for 2 days. ....	43
Figure 4.3: Effect of pitch:solvent ratio on the extraction yield. Experiments were performed at ambient temperature for 30 days with sporadic shaking applied to the mixtures during this period.....	44
Figure 4.4: Boron content of extract and residue of MTP initially spiked with 1000 ppm B after 2 h of reflux extraction with methanol. ....	46
Figure 4.5: ATR spectra of (a) MTP, and its (b) methanol-soluble and (c) methanol-insoluble fractions. MTP fractions were prepared by refluxing 2 g of MTP in 100 ml of methanol for 30 min.....	48
Figure 4.6: ATR spectra of (a) MTP, and (b) its toluene-soluble and (c) toluene-insoluble fractions. MTP fractions were prepared by refluxing 2 g of MTP in 100 ml of toluene for 30 min.....	50
Figure 4.7: ATR spectra of (a) MTP and (b) its benzene-soluble and (c) -insoluble fractions. MTP fractions were prepared by refluxing 2 g of MTP in 100 ml of benzene for 30 min.....	50
Figure 4.8: Solid-state $^{13}\text{C}$ NMR CP MAS spectra of MTP and its methanol-soluble and -insoluble fractions. ....	52
Figure 4.9: Solid-state $^{13}\text{C}$ NMR CP MAS spectra of MTP and its benzene-soluble and -insoluble fractions. ....	53
Figure 4.10: Solid-state $^{13}\text{C}$ NMR CP MAS spectra of MTP and its toluene-insoluble fractions. ....	53
Figure 4.11: $^{13}\text{C}$ NMR data for MTP and its fractions. All fractions were determined by refluxing 2 g of MTP in 100 ml of solvent for 30 min.....	55

Figure 4.12: MALDI mass spectrum of the parent pitch, MTP. The plot shows that MTP is composed largely of compounds in the low molecular mass range. ....	56
Figure 4.13: MALDI mass spectra of the methanol-soluble fractions showing their molecular mass distribution.....	57
Figure 4.14: MALDI mass spectra of the methanol-insoluble fractions showing their molecular mass distribution.....	58
Figure 4.15: MALDI mass spectra of the benzene-soluble fractions showing their molecular mass distribution.....	59
Figure 4.16: MALDI mass spectra of the benzene-insoluble fractions showing their molecular mass distribution.....	59
Figure 4.17: MALDI mass spectra of the toluene-insoluble fractions showing their molecular mass distribution.....	60
Figure 4.18: TMA curve showing determination of the softening point ( $T_s$ ) of raw MTP. ....	64
Figure 4.19: TMA curve showing determination of the softening point ( $T_s$ ) of the methanol-insoluble pitch fraction.....	65
Figure 4.20: TGA curves of raw MTP and its methanol-soluble and –insoluble fractions in $N_2$ . ....	66
Figure 4.21: TGA curves of raw MTP and its benzene-soluble and -insoluble fractions in $N_2$ . ....	67
Figure 4.22: TGA curves of MTP and its toluene-soluble and -insoluble fractions in $N_2$ . ....	68
Figure 4.23: TGA curves showing all soluble fractions having low carbon yield compared with MTP in $N_2$ . ....	69
Figure 4.24: DTG curves of MTP and its insoluble fractions in different organic solvents in $N_2$ . ....	70

## LIST OF TABLES

Table 2.1:	Typical product distribution range of coal tar pitches (Yardim and Ekinci, 2001).....	5
Table 2.2:	Position and assignment of proton ( $^1\text{H}$ ) signals (Zander, 2000) .....	11
Table 2.3:	Position and assignment of carbon ( $^{13}\text{C}$ ) signals (Zander, 2000).....	11
Table 2.4:	Characteristic absorption bands of coal tar pitch and its fractions (Zander, 2000).....	12
Table 2.5:	Estimated use of boron minerals and chemicals in the US (Woods, 1994)	30
Table 4.1:	TMA softening point and elemental analysis of MTP and its fractions.....	47
Table 4.2:	Important MALDI features of MTP and its fractions .....	61
Table 4.3:	Estimation of PAHs and benzo[a]pyrene equivalent, B(a)P, in MTP and its methanol-soluble (MS) and -insoluble (MI) fractions.....	63

## LIST OF ABBREVIATIONS

<b>ATR</b>	Attenuated total reflectance
<b>BCA</b>	Boric acid
<b>BI</b>	Benzene insoluble
<b>BNCT</b>	Boron neutron capture therapy
<b>BPA</b>	2-(Benzyloxy) phenylboronic acid
<b>CP</b>	Cross-polarisation
<b>CP-MAS</b>	Cross-polarisation magic angle spinning
<b>DBA</b>	4-(Dibenzofuranyl) boronic acid
<b>DMF</b>	N,N-dimethylformamide
<b>DMSO</b>	Dimethyl sulphoxide
<b>DTG</b>	Differential thermogravimetry
<b>EHD</b>	2-Ethyl-1,3-hexanediol
<b>Form</b>	Formamide
<b>FTIR</b>	Fourier transform infrared spectroscopy
<b>GC-MS</b>	Gas chromatograph-mass spectrometer
<b>I<sub>ar</sub></b>	Aromaticity index
<b>I<sub>os</sub></b>	Ortho-substitution index
<b>ICP-MS</b>	Inductively coupled plasma mass spectrometer
<b>ICP-OES</b>	Inductively coupled plasma optical emission spectroscopy
<b>IEA</b>	International Energy Agency
<b>MALDI-TOF</b>	Matrix assisted laser desorption/ionisation time of flight
<b>MAS</b>	Magic-angle spinning
<b>MBA</b>	Methyl boronic acid
<b>MeOH</b>	Methanol
<b>MI</b>	Methanol insolubles
<b>MTP</b>	Medium temperature gasifier pitch
<b>m/z</b>	Mass-to-charge ratio
<b>NMR</b>	Nuclear magnetic resonance
<b>PAH</b>	Polycyclic aromatic hydrocarbons
<b>PBA</b>	2-Phenoxyphenyl boronic acid

<b>PBMR</b>	Pebble bed modular reactor
<b>PLA</b>	Phenylboronic acid
<b>Pyr</b>	Pyridine
<b>QI</b>	Quinoline insolubles
<b>Qui</b>	Quinoline
<b>TBA</b>	p-Tolylboronic acid
<b>TCNQ</b>	7,7,8,8-tetracyanoquinodimethane
<b>TG</b>	Thermogravimetry
<b>TGA</b>	Thermogravimetric analysis
<b>THF</b>	Tetrahydrofuran
<b>TI</b>	Toluene insolubles
<b>TMA</b>	Thermomechanical analysis
<b>TOSS</b>	Total side band suppression

# CHAPTER ONE: INTRODUCTION

## 1.1 BACKGROUND

Worldwide, energy demand surpasses supply and South Africa is no exception. The rise in this demand is attributed to various factors such as growing economies, urbanisation and the growing world population. In 2006, the International Energy Agency (IEA) reported that fossil fuel resources supplied about 80% of the world's total energy (IEA, 2006). However, the depletion of fossil fuel resources and increasing levels of greenhouse gases necessitate sustainable and clean ways of producing energy.

Eskom, South Africa's electricity supply utility, is largely a coal-based company, supplying about 90% of the country's electricity. Nuclear energy constitutes about 5% of the energy supply. Eskom is considering nuclear energy for long-term power generation, but the safety of nuclear energy production is a major concern, especially to environmentalists and politicians. The proposed pebble bed modular reactor (PBMR) is a reactor type that meets the required safety standards (Nicholls, 2000).

The PBMR is a graphite-moderated, helium-cooled high-temperature reactor. It uses nuclear-grade graphite. Nuclear-grade graphite consists of chemically pure graphitic carbon and is used primarily in the core of a nuclear reactor to moderate high-energy neutrons to thermal (low-energy) ones. Thermal neutrons are capable of maintaining the nuclear chain reaction within the reactor. Nuclear graphite must be free of neutron-absorbing species such as boron (Kelly, 1981). The removal of impurities prior to the production of nuclear-grade graphite is a vital step (Hall et al., 2006).

Pitches with virtually no impurities are of considerable interest, especially as precursors for advanced carbon materials, e.g. nuclear graphite. Carbon artefacts from coal tar and petroleum pitches find widespread application in many industries. These industries include iron and steel production, construction, the motor industry, nuclear power stations, etc. However, any carbon artefact intended for nuclear applications must meet certain specifications, such as low ash content, high carbon yield and low neutron-

absorbing impurities. In nuclear power plants, carbon artefacts are used in graphite-moderated high-temperature reactors.

Medium-temperature gasifier pitch (MTP) is a by-product of the Sasol-Lurgi coal gasification process (Sima et al., 2003). MTP is a potential precursor for graphitisable carbon. The actual boron content in MTP is low (15 ppm) and this makes accurate determinations difficult. However, the boron content is too high for nuclear moderator applications, which require graphite with less than 1 ppm boron. High-temperature halogen treatments are commonly used to remove impurities from nuclear graphite but there seems to be a limit to the amount of boron that can be removed in this way (Garton, 1957). Solvent extraction at the pitch stage might be a practical proposition for the preparation of low-boron carbons.

## **1.2 AIMS AND OBJECTIVES**

The Carbon Group at the University of Pretoria is trying to produce graphite for nuclear energy applications from local South African raw materials. One of these materials is MTP. This pitch material is a by-product of tar distillation following a coal gasification process, such as the Sasol-Lurgi process. Raw materials of high purity are important, especially as precursors for advanced carbon materials.

The main objectives of the present study were to determine the solubility of MTP in various organic solvents and to study the extraction of boron-containing model compounds using a suitable solvent. The boron content was determined directly from methanol fraction samples and the pitch-rich residues with inductively coupled plasma optical emission spectroscopy (ICP-OES) compatible with organic samples. The analysis was based on the American standard ASTM D 5158-02.

Elemental analysis of MTP and its fractions was done to estimate their aromaticity indices. The presence of characteristic aliphatic and aromatic compounds in MTP and its fractions was determined with infrared spectroscopy (IR) equipped with attenuated total reflectance (ATR). The aromaticity of the fractions was estimated using nuclear magnetic resonance ( $^{13}\text{C}$  NMR). Matrix-assisted laser desorption/ionisation time of flight (MALDI-



TOF) was used to study the molecular weight distribution of MTP and its fractions. Gas chromatography coupled with mass spectrometry (GC-MS) was used to quantify the polycyclic hydrocarbons. The thermal stability of MTP and its fractions was evaluated with thermogravimetry (TG). Softening points were determined with thermomechanical analysis (TMA).

## CHAPTER TWO: LITERATURE REVIEW

### 2.1 PITCH

Pitches are important precursors for carbon materials (Edwards, 1989). They comprise complex mixtures of many individual organic compounds, these being predominantly polycyclic aromatic hydrocarbons and some heterocyclic compounds. There are more than 10 000 organic compounds in pitch according to an older estimate (Zander, 2000). Significant differences in the chemical composition of pitches result from their source.

Pitches are normally obtained by thermal treatment of petroleum and coal fractions. They can also be synthesised by heat treatment of simple aromatic hydrocarbons, e.g. anthracene and naphthalene (Singer et al., 1987, Mochida et al., 2001). Coal tar pitch is obtained by distillation of coal tar. Pitches have higher carbon content and are capable of developing into graphitisable carbons upon heat treatment (Rand et al., 1989, Sima et al., 2003).

Based on their origin, pitches exhibit different properties, e.g. softening point, carbon yield, etc. Almost two-thirds of the compounds that have been separated out from coal tar pitch are polycyclic aromatic hydrocarbons, the remaining fraction being heterocyclic. The separated compounds are composed mostly of three to six aromatic rings, which boil in the range of 340 to 550 °C. Coal tar pitch is composed largely of hydrocarbons, with small amounts of nitrogen, oxygen and sulphur. The degree of aromaticity in the pitch is approximated by the C/H ratio (Rand et al., 1989).

In general, a coal tar pitch has a high carbon yield and a significant amount of quinoline-insoluble fractions. These are quinoline-insoluble residues, i.e. solid carbon particles found in coal tars following a carbonisation/coking process (Ball, 1978). In general, petroleum-derived pitches have a low carbon yield upon heat treatment and fewer quinoline insolubles (Zander, 2000). Sections 2.2 and 2.3 focus on coal tar and petroleum-derived pitches respectively.

## 2.2 COAL TAR PITCHES

The conversion of coals by pyrolysis to produce coke, a highly carbonaceous material, results in coal tar as by-product. Distillation or thermal treatment of coal tar results in coal tar pitch. The coal tar pitch comprises mostly aromatic hydrocarbons with some alkyl substituted groups, for instance methyl groups (Rand et al., 1989). These pitch materials may exhibit different characteristics depending mainly on their original source and processing temperature (Yardim et al., 2001, Mokoena et al., 2008).

Generally, coal tar pitches have a higher carbon yield on carbonisation than petroleum-derived pitches (Zander, 2000). These coal-derived pitches have high boiling points of around 550 °C. Coal tar consists mostly of carbon and hydrogen, with a small amount of heteroatoms. Table 2.1 lists the typical product distribution of coal tar pitches.

**Table 2.1:** Typical product distribution range of coal tar pitches (Yardim and Ekinci, 2001).

Product	Boiling range, °C	Weight %
Light oil	<150	1
Naphthalene oil	195–230	12
Creosote oil	230–300	6
Anthracene oil	>300	20
Pitch	residue	60
Tar acids		1

Medium-temperature gasifier pitch (MTP) is a coal tar pitch that is produced by the Sasol-Lurgi process of coal gasification (Sima et al., 2003, Mokoena et al., 2008). Pitch transforms by means of delayed coking into carbon. Tar pitches differ remarkably in their characteristics, such as their solubility in different organic solvents, carbon yield, softening point, viscosity, etc. These characteristics have a profound impact on both the commercial and technological application of pitches. It is therefore important to modify pitches prior to their industrial applications.

Several methods, such as heat treatment in inert or oxidative atmospheres (Mokoena et al., 2008a) and solvent fractionation (Zander, 2000), can be used to modify pitches. Some pitch fractions can be removed (Yardim et al., 2001) by solvent extraction or by means of vacuum distillation prior to thermal treatment. Medium-temperature pitches are potential precursors of carbon materials (Sima et al., 2003) and their characterisation has attracted enormous interest from both the scientific and commercial viewpoints.

### **2.3 PETROLEUM PITCHES**

Petroleum pitch is obtained by low-pressure and low-temperature cracking of steam cracker tar. Petroleum pitch precursors include naphtha and gas oils. The conversion of petroleum pitch precursors to petroleum pitch follows a number of chemical processes. These raw materials can be processed via heat treatment, oxidation, vacuum or steam stripping or simple distillation. The chemical nature of petroleum pitches is chiefly dependent on their origin and the processing methods used, e.g. thermal treatment and processing temperature. Petroleum pitches are generally less aromatic than coal tar pitches. When petroleum pitches are subjected to heat treatment for longer times, the result is aromatic pitches with improved anisotropic content (Rand et al., 1989).

Thermal treatment of petroleum pitches to around 1000 °C, in an inert atmosphere, gives petroleum coke. Petroleum coke is an important feedstock of nuclear-grade graphite. Calcined petroleum cokes are broken into smaller pieces and screened to produce coke particles with one long dimension. Coke particles produced this way are called needle cokes. These cokes are then mixed together with pitch and extruded to form carbons. The formed carbons are aligned parallel to the extrusion axis and have anisotropic properties (Gillin, 1967).

### **2.4 CHARACTERISATION OF PITCH**

Pitches are used in the manufacture of various materials, such as engineering carbon and graphite (Rand, 2001). Pitch, which is readily available and cheap, is an important source of graphitisable carbon (Rand, 2001, Sima et al., 2003). Various techniques have been used for the characterisation of a pitch owing to its complex nature. The solubility of

pitch in organic solvents has been and still is the technique mostly commonly used for the characterisation of pitches. These techniques are used to characterise the raw pitch and its chemical changes after thermal treatment. They provide useful information (Zander, 2000). In the following subsections, however, the focus is more on the solubility of pitch in organic solvents, solvent fractionation, nuclear magnetic resonance (NMR) spectroscopy and infrared spectroscopy (IR).

### 2.4.1 Solubility

Several reasons led (Guillén et al., 1991) to study the extractive capacity of organic solvents with pitches. The following are some of the reasons:

- (i) Old solvent fractionation methods were being used to study the nature and constituents of pitches.
- (ii) The ability of some of organic solvents, e.g. toluene and quinoline, to dissolve pitch is very important for the industrial application of pitches.
- (iii) The application of analytical techniques, e.g. gas chromatography, mass spectroscopy and NMR spectroscopy, requires that pitch be dissolved in suitable organic solvents.
- (iv) The progression of heat treatment processes in pitches should be studied by assessing the degree of extraction of pitches with organic solvents.
- (v) Assessment of the quality of pitch as a carbon precursor can also be achieved by solvent extraction of pitch.

(Guillén et al., 1991) found that there was no correlation or reaction between pitch components and the solvents. It was also found that there was no simple relationship between the solubility of coal tar pitch and solvent properties such as dipole moment, dielectric constant or solubility parameter. Solubility parameters can be used to try to understand the solubility of pitches.

Due to increasing interest in the behaviour of pitch with solvents, Guillén and co-workers (1991) studied the extractive ability of 27 organic solvents with coal tar pitches. The

reproducibility of the data for these solvents was also studied using an ultrasonic bath. The behaviour of pitches and their solubility in organic solvents could be explained by the Hildebrand solubility parameter. The term ‘solubility parameter’ was first coined by Hildebrand and Scott (Barton, 1983). The Hildebrand solubility parameter is defined as the square root of the cohesive energy density:

$$\delta = \sqrt{\frac{\Delta U}{V}}, \quad (2.1)$$

where  $\delta$  is the solubility parameter,  $\Delta U$  is the energy of the vaporisation and  $V$  is the molar volume of the compound (Barton, 1983, Blanco and Guillén, 1991). Initially, the Hildebrand solubility parameter was specially designed for non-polar and non-associating systems. The concept has since been expanded further to incorporate polar systems (Levin and Redelius, 2008).

Hansen’s solubility parameter includes dispersive interactions ( $\delta_d$ ), polar interactions ( $\delta_p$ ) and hydrogen-bonding interactions ( $\delta_h$ ) (Levin and Redelius, 2008). Hansen’s three-dimensional solubility parameter theory states that cohesive intermolecular forces can be understood as the sum of  $\delta_d$ ,  $\delta_p$  and  $\delta_h$ . It can be expressed as:

$$\delta = \sqrt{\delta_d^2 + \delta_p^2 + \delta_h^2} \quad (2.2)$$

#### 2.4.2 Solvent fractionation

One of the earliest methods for pitch characterisation was determining the solubility of pitch in organic solvents, i.e. solvent fractionation. Solvent fractionation is still a method of choice among pitch workers. It is now used to modify the chemical structure of the pitch before and after fibre processing (Rand et al., 1989).

Solvent fractionation is routinely used for pitch purification. The pitch is first dissolved in a suitable organic solvent and extracted with another solvent, which is immiscible with the first solvent. Purification of a precursor pitch depends largely on the final industrial application. For example, if the pitch were intended for the production of nuclear graphite, it would be necessary and important to rid it of neutron-absorbing species such

as boron. Purification of pitch, i.e. removal of inorganic material, was achieved with solvents such as toluene and toluene-hexane mixture (Lim and Lee, 1991).

The following solvents normally fractionate coal tar pitches used in thermal heat treatment industries: quinoline and pyridine, benzene and toluene, petroleum ether and *n*-hexane. Even so, discrepancies in naming both soluble and insoluble components in these solvents were reported (Rand et al., 1989). Quinoline/pyridine-insoluble fractions are solid impurities and aromatic compounds of high molecular weight. These fractions are also called  $\alpha$ -resins or  $C_1$  components.  $\beta$ -resins or  $C_2$  components are insoluble in benzene or toluene but soluble in quinoline or pyridine. The resinoid fraction is a material that is soluble in benzene or toluene but insoluble in petroleum ether or *n*-hexane. Crystalloid is a pitch component that is soluble in petroleum ether or in *n*-hexane (Rand et al., 1989).

The solubility of pitch in organic solvents depends on the following structural features (Zander, 2000):

- (i) Molecular weight
- (ii) Structure (topology)
- (iii) Functional groups
- (iv) Geometry, e.g. deviation from planarity

Planar polycyclic aromatic compounds are poorly soluble in organic solvents. However, non-planar molecules with the same molecular weight exhibit a high degree of solubility. Powerful solvents for pitches such as quinoline and toluene are expected to dissolve largely non-planar polycyclic aromatic pitch components.

The solubility of large planar polycyclic aromatic compounds depends largely on molecular weight and to a lesser extent on the structure. It decreases with an increase in molecular weight (Zander, 2000, Lavin, 2001). Therefore, it can be said that pitch fractions that are insoluble in powerful solvents are composed mostly of planar polycyclic aromatic compounds (Zander, 2000). Benzene and toluene are some of the organic solvents that do not dissolve the mesophase-forming fraction of an isotropic

pitch. Consequently, separation of the mesophase-forming fraction can be achieved by solvent fractionation (Lim and Lee, 1991). Stefano et al. (1995) reported that the quinoline-soluble, benzene-insoluble coal tar pitch component is very important for mesophase formation.

### 2.4.3 Nuclear magnetic resonance

$^1\text{H}$  and  $^{13}\text{C}$  nuclear magnetic resonance (NMR) spectroscopy can be used to obtain statistical information on the structure of pitch.  $^1\text{H}$  NMR has been widely used to obtain the distribution of protons from the different environments in the pitch (Zander, 2000). The different chemical environments include aromatic hydrogen, olefinic hydrogen, and hydrogen found in the  $\alpha$ ,  $\beta$  and  $\gamma$ -aliphatic groups. Table 2.2 gives typical ranges of band positions ( $\delta$ , ppm).  $^{13}\text{C}$  NMR spectroscopy has been widely used to determine the carbon skeleton of coal tar pitches. Skeletal carbon information on low volatile materials derived from petroleum can also be obtained (Fischer et al., 1978).  $^{13}\text{C}$  NMR spectroscopy is used to determine true values for aromaticity and the percentage of the quaternary aromatic carbon of the whole material. The extent of condensation of the main polycyclic aromatic structures present in the material is measured by the quaternary aromatic carbon (Zander, 2000). Table 2.3 lists the  $^{13}\text{C}$  NMR shift ranges ( $\delta$ , ppm) of carbon resonances as a representative carbon skeleton of pitches.



**Table 2.2:** Position and assignment of proton ( $^1\text{H}$ ) signals (Zander, 2000).

Range of signal ( $\delta$ , ppm)	Assignment and symbol
6.2–9.2	Aromatic, $\text{H}_{\text{Ar}}$
4.5–6.0	Olefinic, $\text{H}_{\text{olefinic}}$
1.7–4.4	Aliphatic, $\text{H}_{\alpha}$ ( $\alpha\text{-CH}_2$ , $o\text{-CH}_2$ , $\alpha\text{-CH}_3$ , benzylic)
1.0–1.7	Aliphatic, $\text{H}_{\beta}$ ( $\beta\text{-CH}_2$ tetralins, $\beta\text{-CH}_2\text{-indans}$ , $\beta\text{-CH}_3$ , remote $\text{CH}_2$ , $\beta\text{-CH}_2$ alicyclics)
0.7–1.0	Aliphatic, $\text{H}_{\gamma}$ , (remote $\text{CH}_3$ )

**Table 2.3:** Position and assignment of carbon ( $^{13}\text{C}$ ) signals (Zander, 2000).

Range of positions ( $\delta$ , ppm)	Assignments
110–150	Aromatic
18–23	$\delta\text{-CH}_3$
13–15	Remote $\text{CH}_3$
33–42	$\text{CH}_2$ , benzylic ( $\text{Ar-CH}_2\text{-Ar}$ , meso-dihydro-aromatics)
29–31	$\text{CH}_2$ , (9,10-dihydro-phenathrene type, tetralin $\delta$ -position type)
24–26	$\text{CH}_2$ , (tetralin $\beta$ -position type)

#### 2.4.4 Infrared spectroscopy

Infrared spectroscopy (IR) has been widely used to characterise pitch samples, both soluble and insoluble fractions. However, there are inherent limitations concerning the application of IR to characterise pitch materials due to their complex nature. However, the most important functional groups present in the pitch, i.e. aromatic hydrogen, aromatic carbon, carbonyl and carboxylic groups and aliphatic hydrogen, can be identified. In addition, the extent of aromatic substitution can be approximated by determining aromaticity and ortho-substitution indices. These indices can be calculated from absorbance or band areas in the spectra (Menéndez et al., 2000).

Coal tar pitch and its fractions, which were obtained by solvent fractionation, have been characterised using IR spectroscopy. It was generally concluded, inter alia, from the data gathered that the most condensed aromatic structures are found in the insoluble fractions of pitch. Aromatic hydrogen was found in most cases in structures comprising four neighbouring C–H groups (Guillén et al., 1992). Diffuse reflectance spectroscopy can be used for characterisation of these complex materials; transmission spectroscopy does not give a signal when used. Coupling Fourier transform infrared spectroscopy (FTIR) with techniques such as photo-acoustic or diffuse reflectance spectroscopy can greatly enhance the resolution (Menéndez et al., 2000).

**Table 2.4:** Characteristic absorption bands of coal tar pitch and its fractions (Zander, 2000).

Band position (cm <sup>-1</sup> )	Assignment
3400–3600	Hydroxyl group (–OH)
3050	Aromatic C–H stretching
2920	Aliphatic C–H stretching
1720, 1700, 1654, 1648	C=O vibration modes
880, 840, 814, 750	Aromatic C–H out-of-plane vibration frequencies

880 cm<sup>-1</sup>: isolated C–H bonds (type: 9,10-position in anthracene); 814 cm<sup>-1</sup>: two or three adjacent C–H bonds (type: 9,10-position in phenanthrene, pyrene); 750: four adjacent C–H bonds (type: terminal rings)

## 2.5 THERMAL TREATMENT OF PITCHES

Pitches must first be subjected to high-temperature treatment before being transformed into high-performance carbon materials. Heat treatment is performed under an inert atmosphere. Low molecular weight species escape as volatiles and the carbon yield of the residue increases. The formation of large polycyclic aromatic hydrocarbons (PAHs) during heat treatment of pitches is due, among others, to thermal decomposition and polymerisations reactions. These reactions are accompanied by the release of volatile compounds and the orientation of PAHs in the preferred orientation. The preferred alignment of PAHs gives rise to an optically anisotropic phase which grows from an isotropic matrix (Montes-Morán et al., 2002).

### 2.5.1 Mesophase

Heat treatment of various pitches to temperatures in the range of 300–500 °C, under an inert atmosphere, results in an optically anisotropic mesophase (Brooks and Taylor, 1965). The mesophase grows from an isotropic matrix and is made up of nematic, discotic planar aromatic liquid-crystalline spheres (Moriyama et al., 2000). These spheres develop and grow according to the fundamental processes of nucleation. Nucleation is a generation step, leading to the growth and coalescence of spheres (Moriyama et al., 2004).

The growth of mesophase spheres is influenced by changes in the viscosity of the system. As the spheres grow, they coalesce and develop into a bulk mesophase (Montes-Morán et al., 2002). Bulk mesophase is a continuous anisotropic phase which maintains some degree of fluidity (Fitzer et al., 1995). The term ‘mesophase’ is derived from a Greek word *mesos*, which means intermediate. It refers to spheres and mosaic of a material before they solidify (Brooks and Taylor, 1965). Mesophase is a general description for a range of materials of distinct viscosities and macro-crystallinity (Marsh et al., 1999).

Figure 2.1 depicts a proposed Spider Wedge model of mesophase which shows aromatic units with diameters in the range 0.6 to 1.5 nm (Mochida et al., 2000). These aromatic units have high molecular weight, i.e. 400–4000 atomic mass units. They are connected

by phenyl-phenyl or methylene bridges. Phenyl- and methylene groups are important for the solubility and fusibility of mesophase components.

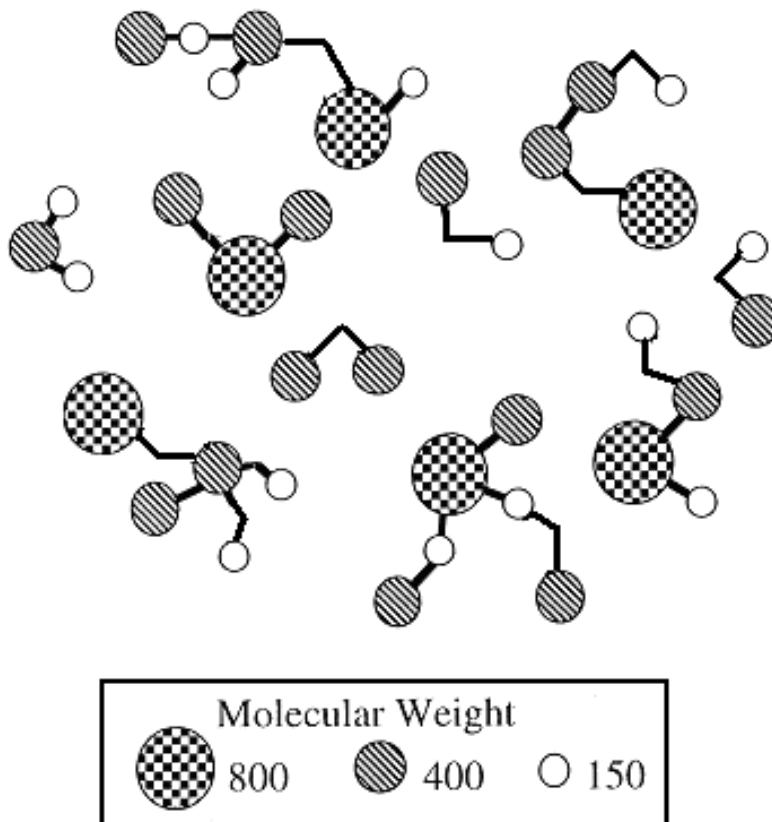


**Figure 2.1:** Spider Wedge model of mesophase constituent molecules (Mochida et al., 2000).

Mesogens are the basic components of the liquid crystals and they bring about structural stability in the liquid crystals. Mesogens have a substantial polarity such as in the hydroxyl, nitrile, carboxylic groups and so on. Representative mesogen components in different mesophase pitches are shown in Figure 2.2. Mesogens are also characterised by metallic groupings and their extensive aromaticity.

Mesogen structures occur in a linear (rodic) shape or are shaped like discs, i.e. ‘discotic’, with the latter shape being more effective for self-assembly (Marsh et al., 1999). The two mesogenic shapes are illustrated in Figure 2.3. The distortion of a mesophase ‘structure’ by mechanical means and its partial recovery give mesophase its plastic behaviour. The capability of mesophase to be deformed and its viscosity are important features that make it usable (Marsh et al., 1999). The distortion of bulk mesophase can be achieved in the temperature range up to 430 °C (Fitzer et al., 1995).

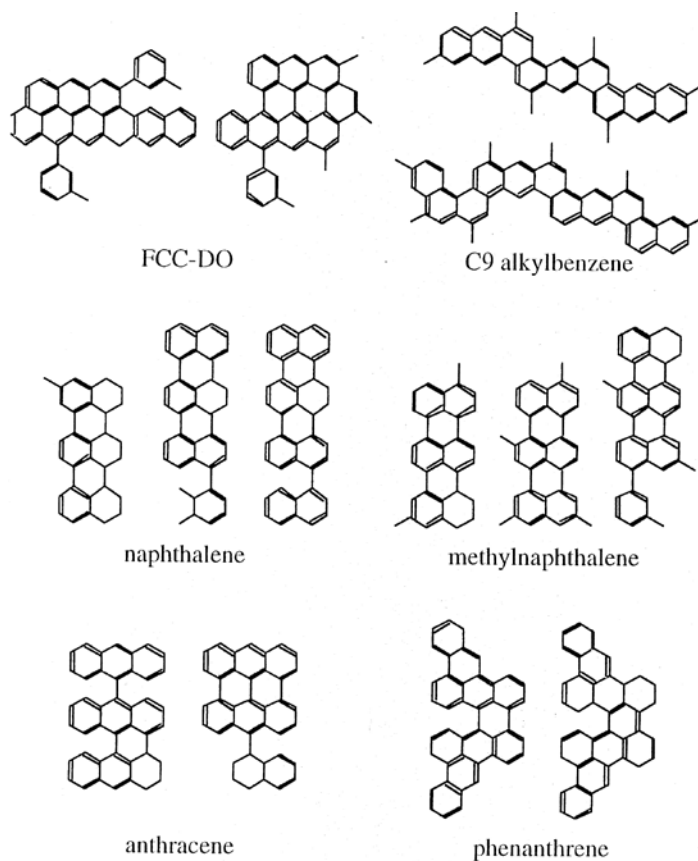


**Figure 2.2:** Typical mesogen units in different mesophase pitches (Mochida et al., 2000).

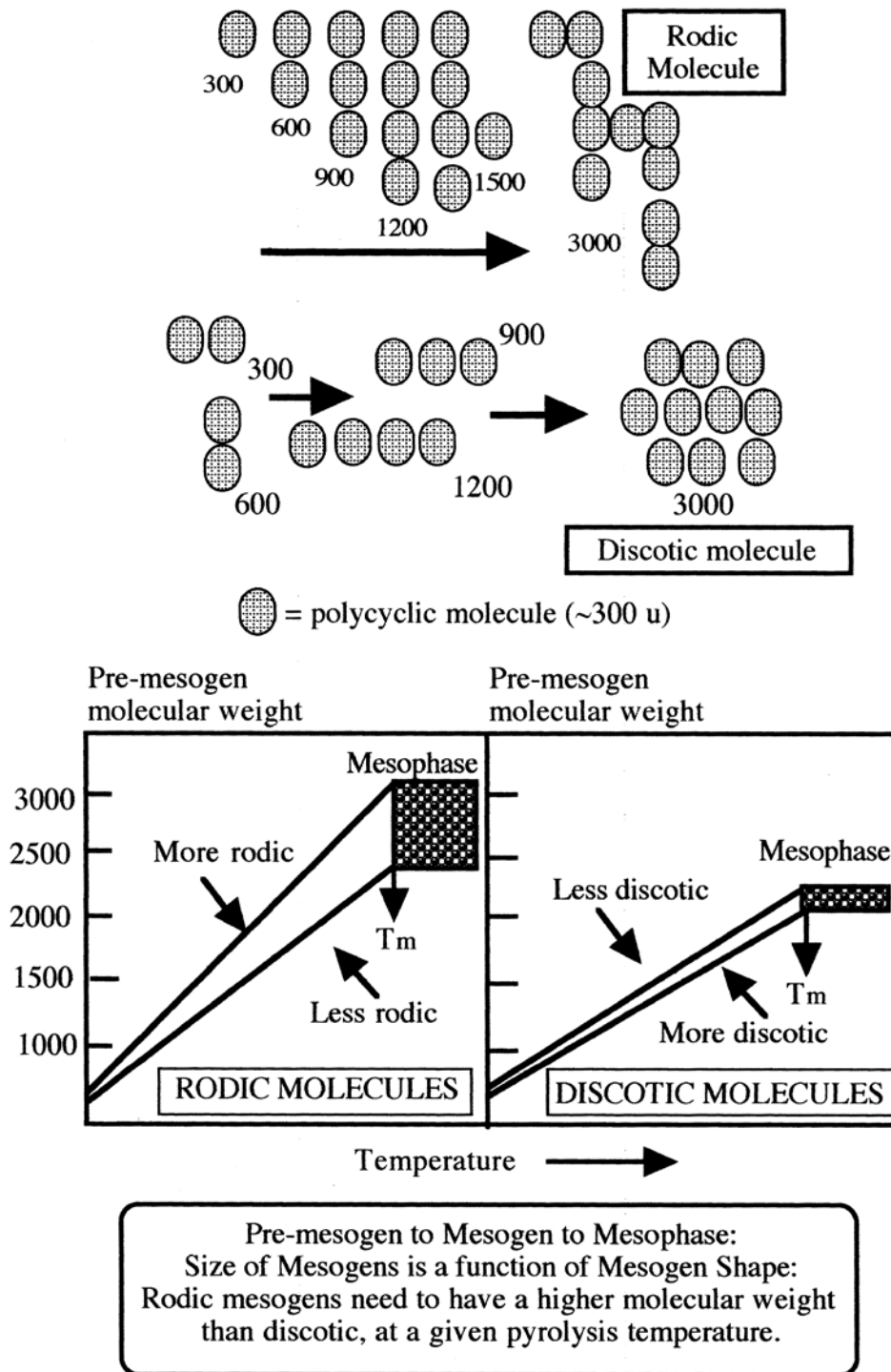


**Figure 2.3:** Relationships between rodic and discotic shapes of mesogens in terms of temperature of formation of mesophase (Marsh et al., 1999).

## 2.5.2 Carbonisation

Carbonisation is the transformation of a carbonaceous material by thermal treatment into a carbon-rich solid residue (Fitzer et al., 1995). This process is carried out in an inert environment. Carbonisation, like many other thermal processes, is not a simple process as it involves many reactions. The thermal reactions that normally take place during carbonisation include hydrogen transfer, hydrogen removal, condensation and isomerisation (Singer et al., 1987). The rate of carbonisation is much faster than that of coalification by many orders of magnitude. The two processes differ in that regard.

Fitzer et al. (1995) define coalification as “a geological process of formation of materials with increasing content of the element carbon from organic materials that occurs in a first biological stage into peats. This is followed by a gradual transformation into coal by action of moderate temperature (227 °C) and high pressure in a geological stage.” The extent of carbonisation and the residual content of foreign elements are dependent on the final heat treatment temperature applied. High carbon contents of the residues, i.e. 90–99 wt % can be obtained in the temperature range 927–1327 °C (Fitzer et al., 1995).

Cokes of comparatively high yields are formed from liquid phases of petroleum-derived and coal tar pitches. The formation of liquid phases follows thermal treatment of both types of pitch. The energies of dissociation of aromatic C–C bonds are higher than those of aromatic C–H bonds. Hence, pitches are able to form cokes upon high-temperature treatment. In contrast, thermal treatment of aliphatic hydrocarbons to high temperatures leads mostly to disintegration. The aliphatic materials disintegrate because the dissociation energies of aliphatic C–C bonds are lower than those of C–H bonds. Thermally induced development of cokes is favoured by large C/H ratios, i.e. high carbon content of pitches (Zander, 2000).

Blanco and co-workers (2002) studied the behaviour of various fractions from the optical texture of cokes formed during carbonisation. They found that cokes from both isotropic and anisotropic phases are distinct. The latter exhibited needle-like structures with an optical texture of flow domains. The coarse mosaics and small domains that were observed in cokes from parent pitch were also seen in cokes from anisotropic pitch. The

reduction in optical texture of cokes from anisotropic phases could be attributed to increasing viscosity and the high concentration of primary quinoline insolubles (QI). The presence of QI impedes the formation of large domains.

When pitches are subjected to high-temperature treatment, their constituents pass through different reaction pathways. Information on the reaction pathways can be obtained by studying the carbonisation chemistry of model compounds, especially polycyclic aromatic hydrocarbons (Lewis, 1982). It must be borne in mind that a pure thermally reacting hydrocarbon is a much less complex system than a thermally reacting pitch (Zander, 2000).

The development of optical anisotropy in the resultant coke is somewhat influenced by the molecular structure of the carbonisation intermediates. The carbonisation intermediates have been identified in the thermal treatment of acenaphthylene. The pyrolysis of this chemical compound presents an uncommon example of atmospheric carbonisation of a pure compound (Mochida et al., 2001).

The carbonisation model of acenaphthylene is shown in Figure 2.4. The intermediates marked II, III and VI are suggested formulas based on chemical analyses. The interaction among the carbonisation intermediates is shown by the carbonisation reactivities of acenaphthylene (I) and decacyclene (VI). Decacyclene is invariably found during thermal treatment of acenaphthylene as an intermediate and is stable on its own, even at 500 °C. Acenaphthylene, on the other hand, forms optical anisotropy largely at lower thermal treatment temperatures. These findings suggest that reactive intermediates, which are not included in the single thermal treatment of decacyclene, have an important role. A small constituent at the intermediate steps of carbonisation can have an effect on the final properties of a coke (Mochida et al., 2001).



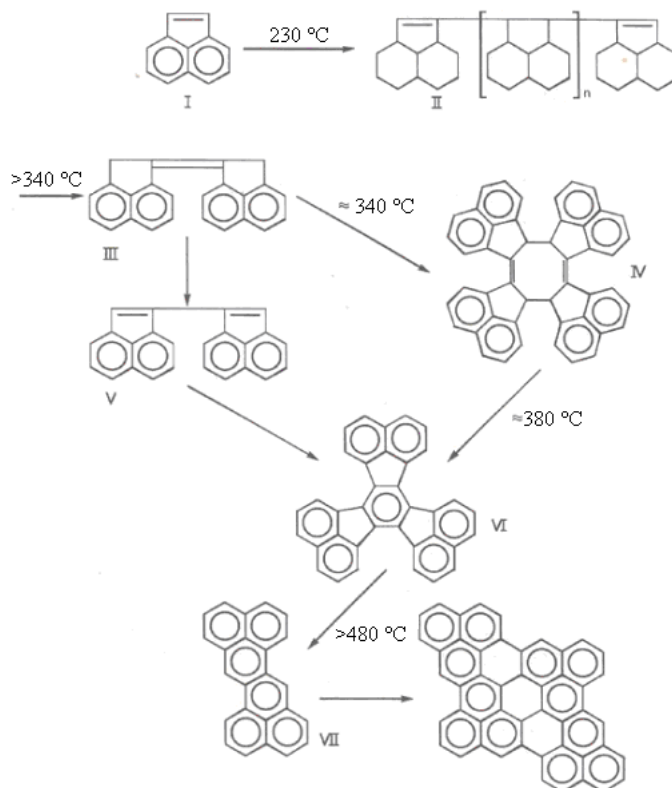


**Figure 2.4:** A carbonisation model of acenaphthylene showing molecular size enlargement of aromatic systems (Mochida et al., 2001).

### 2.5.3 Graphitisation

Carbons can be prepared from various precursor materials. These materials include chemically pure compounds and mixtures of broad molecular weight compounds, e.g. pitches. The ordering of carbon materials is greatly enhanced by increasing heat treatment temperatures (Kelly, 1981). Fitzer et al. (1995) defined graphitisation as “a solid-state transformation of thermodynamically unstable non-graphitic carbon into graphite by means of heat treatment.” It is therefore incorrect to use the term *graphitisation* to refer to a thermal treatment above  $2230\text{ }^{\circ}\text{C}$  of carbonaceous materials without any accompanying ordering or crystallinity of the material.

According to Kelly (1981), graphitisation should be understood as two processes taking place one after the other. First, a starting material transforms into a solid carbon (coke) and various volatile compounds. Conversion of carbon to graphite is the next step.

Kelly's first process has, however, been described by many authors as carbonisation (Fitzer et al., 1995, Oberlin and Bonnamy, 2001).

The graphitisation process is a transformation of carbonaceous materials characterised by their turbostratic order and a progressive 3D ordering of layers as heat treatment increases to above 2400 °C. Bourrat (2000) introduced the concept of turbostratic order in graphitic carbons. Each turbostratic group comprises a number of graphite layers stacked together roughly parallel and equidistant, but with each layer having a completely random orientation about the layer normal.

The observation that heat treatment of materials that have turbostratic structures was accompanied by a progressive 3D ordering of the layers was made by Franklin (1951). This was seen by many as a decisive contribution in the field of carbon (Fitzer et al., 1995). The ordering of perfect graphite-like 3D structures is not the only feature of the graphitisation process, which is also the perfection of defects within the grapheme layers. Again, Franklin proposed three different types of carbon: graphitising carbons, non-graphitising carbons and carbons that graphitise partially. The models for these different types of carbon are depicted in Figure 2.5.

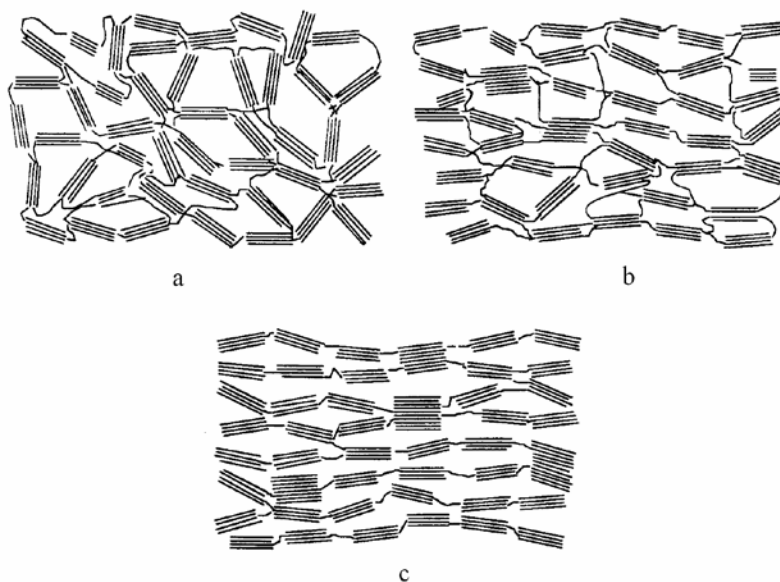


**Figure 2.5:** Models for different structures of carbons proposed by Franklin (1951); (a) non-graphitising, (b) partially graphitising and (c) graphitising carbons.

During the graphitisation process, a solid carbonaceous material undergoes a homogeneous qualitative transformation, with a growing number of layer pairs reaching a graphite order (Oberlin and Bonnamy, 2001). A graphite order is a measure of arrangement of the graphene layers. It is given by the equation  $d_{002} = c/2$ , where  $d_{002}$  is the interlayer spacing between 002 layers, and  $c$ , which equals 670.8 pm, is the lattice constant of the hexagonal unit of graphite. The interlayer spacing progressively reduces from 344 pm to an eventual graphite value of 335.4 pm during graphitisation (Bourrat, 2000). The hexagonal unit of structure of graphite is shown in Figure 2.6.

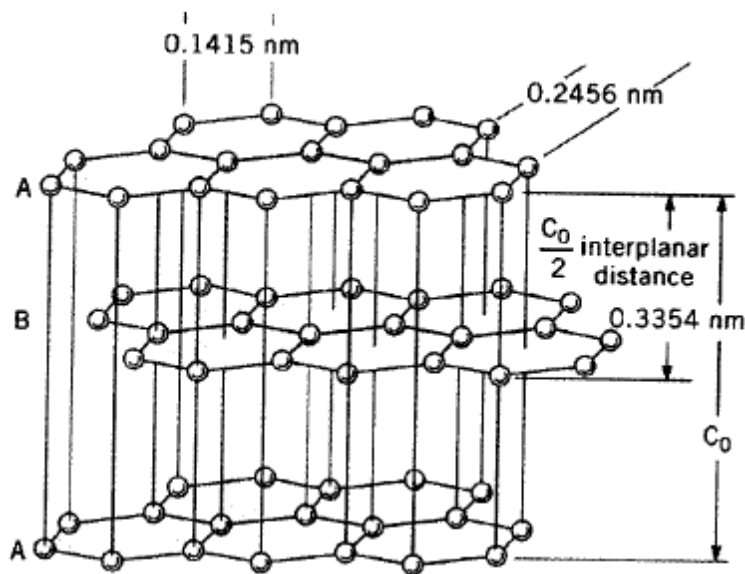


**Figure 2.6:** Hexagonal unit of structure of graphite showing the  $d_{002}$ -spacing (Kirk-Othmer, 2005).

Graphene layers must reach a near-perfect 2D structure prior to 3D ordering of the carbon material. Increasing heat treatment temperature not only improves the 3D ordering of carbon material, but also removes the defects within the material. Therefore, the transformation that takes place within the layer itself is vital for the progress of graphitisation.

Heteroatoms, oxygen, nitrogen and sulphur atoms are primary kinds of defect found in carbon precursor materials. These heteroatoms, part of which are removed during carbonisation (Oberlin and Bonnamy, 2001), remain trapped in the carbon structure up to

temperatures around 2200 °C. The progress of graphitisation is controlled largely by the annealing out of defects and the removal of interstitial carbon (Bourrat, 2000). The loss of minor atoms, e.g. heteroatoms, from aromatic structures during the graphitisation process creates openings and empty spaces in the planes. These spaces are filled by the movement of carbon atoms from above and below the planes until a perfect 3D crystalline graphitic structure is obtained (Brooks and Taylor, 1965).

## **2.6 EFFECT OF BORON ON GRAPHITISATION**

The graphitisation process depends largely on high-temperature heat treatment and annealing out of defects from aromatic structures. However, the degree of graphitisation of aromatic carbons can be enhanced by the catalytic effect of boron (Eichner et al., 1996, Frackowiak et al., 2001). Murty et al. (1977) studied the catalytic effect of boron on three different carbon materials. The presence of boron accelerated the graphitisation rate for the three carbon materials. Boronated carbons attained, at concentration levels of 0.5 and 1 wt % B, lattice constants the same as those of carbons without boron. This was achieved at temperatures lower than the usual graphitisation temperatures.

Boron as a substitution element plays a vital role in carbon materials. Boron compounds in the carbon matrices, when heat treated together, are known to increase the crystallinity of the carbon materials (Hamada et al., 2002). The mechanical stability, thermal conductivity, oxidation resistance and structural properties of carbon materials have all shown improvement in the presence of boron (Eichner et al., 1996, Becker et al., 1999, Frackowiak et al., 2001). These properties are especially important for carbon materials manufactured, particularly for use in high-temperature nuclear reactors. The flexural strength and strain to failure of carbon materials were also improved by boron (Carreira et al., 2003).

Boron increases electrochemical properties, such as capacity and efficiency, when incorporated into graphitic material for Li-ion battery anodes (Carreira et al., 2003). All these properties are enhanced owing to the  $sp^2$  nature of boron which makes its inclusion into discotic nematic liquid crystals possible (Rand et al., 2001). Boron incorporation into

the discotic nematic liquid crystalline matrix is achieved with a relatively small disruption of the carbon matrix.

## 2.7 BORON REMOVAL METHODS

The boron content of MTP may limit its use as a precursor for nuclear carbon. Pitch precursors with fewer impurities are important for the fabrication of advanced carbon materials such as nuclear graphite. One of the specifications for nuclear-grade graphite is the low boron equivalence, i.e. 2 ppm. Purification of MTP at the pitch phase is a desired option compared with conventional high-temperature purification of graphite.

This section presents different studies found in the literature on boron removal from various materials other than pitches. Ayers et al (1981) studied the solvent extraction of boron with a mixture of two organic solvents. They reported on the feasibility of reducing boron concentration to low ppm levels using an admixture of 2-ethyl-1,3-hexanediol and 2-chloro-4-(1,1,3,3-tetramethylbutyl)-6-methylol-phenol. Sah and Brown (1997), in their review article, reported on the use of organic solvents for boron extraction. In its organic complexes, boron can be extracted as boron-2-ethyl-1,3-hexanediol (EHD) complex into chloroform or benzene and as 2,4-dinitro-1,8-naphthalenediol boron complex in toluene. The removal of boron with EHD compares favourably with the other complexes owing to its simplicity, ease of use and high extraction coefficient (Ramanjaneyulu et al., 2008).

Boron can also be separated into isopentanol as a complex with a 24% solution of 2,4-dimethyl-2,4-octanediol (Sah and Brown, 1997). Extraction of boron as methyl borate complex by distillation has also been reported (Boltz and Howell, 1978, Yoon and Kim, 1985). Solvent extraction has been utilised for the determination of small amounts of boron in steel (Pasztor et al., 1960, Ishii et al., 1984).

Ramanjaneyulu et al (2008) reported 80% boron recovery from standard boric acid solutions. The efficacy of Amberlite IRA-743, an ion-exchange resin for the removal of boron from geothermal waters, was discussed in detail by Xu and Jiang (2008). Amberlite IRA-743 is specially manufactured for boron removal and offers high selectivity for boron. This high boron selectivity by Amberlite IRA-743 is due to

*N*-methylglucamine functional groups attached to the macroporous polystyrene matrix. Boron can be extracted from organic material with a Parr bomb technique (Williams et al., 2001).

## 2.8 BORON DETERMINATION METHODS

Determination of low boron concentrations from different materials, ranging from brine to nuclear material, is important in various industries (Coedo et al., 1993, Gazi et al., 2008, Ramanjaneyulu et al., 2008, Rao and Aggarwal, 2008, Thangavel et al., 2004). A lot of work has been done on the separation of boron from different materials. Various reagents have been used to form complexes with boron for its trace determinations. However, the best method depends on the sensitivity and stability of the complex. The analyte of interest in complexes can be efficiently determined using photometric techniques. When a ligand is stabilised, an intensive colour develops. A complexed element plays no role in the position and intensity of the spectrum. A good example is that of curcumin and its boron complex; the latter exhibits the same absorption patterns as the former.

### 2.8.1 Curcumin

Curcumin is a very sensitive, widely applied organic reagent for the determination of boron concentration. This organic reagent derives its name from curcuma or turmeric. Curcuma is a horizontal stem of a tropical species (Boltz and Howell, 1978). Curcumin is the most important component (curcuminoid) of turmeric. It can serve as both a spice in curry and a pigment in yellow mustards, cosmetics, pharmaceuticals and hair dyes (Boltz and Howell, 1978, Payton et al., 2007). Turmeric belongs to the ginger family, *Zingiberaceae*. Curcuminoids, which are polyphenols, give turmeric its yellowness. Two tautomeric forms of curcumin are enol and keto, with the former being the most energetically stable of the two forms. The enol tautomer is stable in both the solid phase and in solution. Studies of the structure of curcumin in solution show that it exists as a keto-enol tautomer (Payton et al., 2007). The structural form of curcumin is shown in Figure 2.7.

The reaction of boric acid and curcumin results in two distinct red dyes, namely rosocyanine and rubrocurcumin, depending mainly on the absence or presence of oxalic acid. A curcumin protonated by a mineral acid combines with boric acid to form rosocyanine. The reaction is somewhat slow and is limited by the presence of water. Rosocyanine is a 2:1 curcumin-boron complex with intrinsically higher molar absorptivity than rubrocurcumin (Boltz and Howell, 1978). The molar absorptivity coefficient for rubrocurcumin is  $73.6 \times 10^3 \text{ L mol}^{-1} \text{ cm}^{-1}$  and for rosocyanine it is twice as large (Perkampus, 1992). The structure of rosocyanine is shown in Figure 2.8.

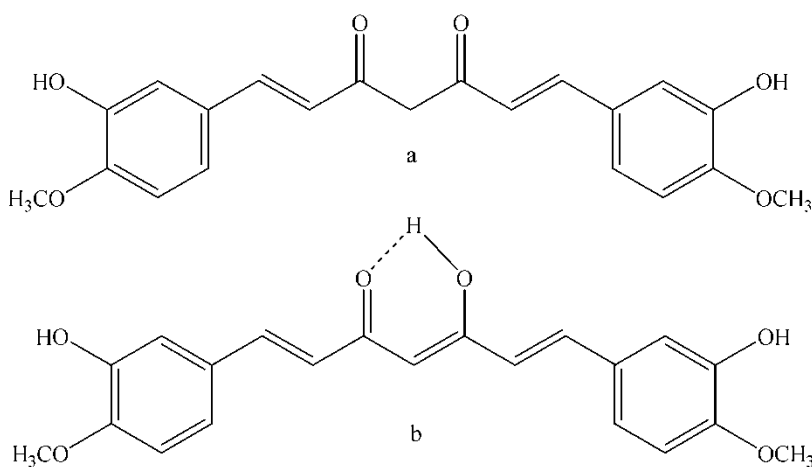


**Figure 2.7:** Structural forms of curcumin: (a) keto and (b) enol isomers. Curcumin is a chemical compound that can be used for quantifying boron (Iwunze, 2004).

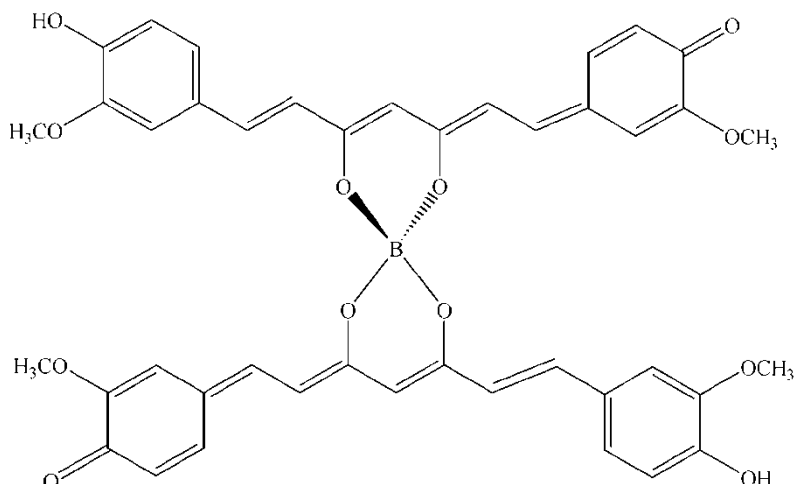


**Figure 2.8:** Structure of rosocyanine, a curcumin-boron complex (Uppström, 1968). Curcumin reacts with boric acid to give a red complex, rosocyanine.

Rubrocurcumin is a red complex, which forms preferentially in the presence of oxalic acid. It is a complex of curcumin, boric acid and oxalic acid. Maximum colour development for the complex is achieved by evaporating the reaction mixture to dryness. The presence of water impedes the formation of rubrocurcumin, while the presence of a mineral acid could result in the formation of rosocyanine (Boltz and Howell, 1978). Rubrocurcumin and rosocyanine are distinct because rubrocurcumin is a neutral molecule and rosocyanine comprises ions. The structure of rubrocurcumin is shown in Figure 2.9.

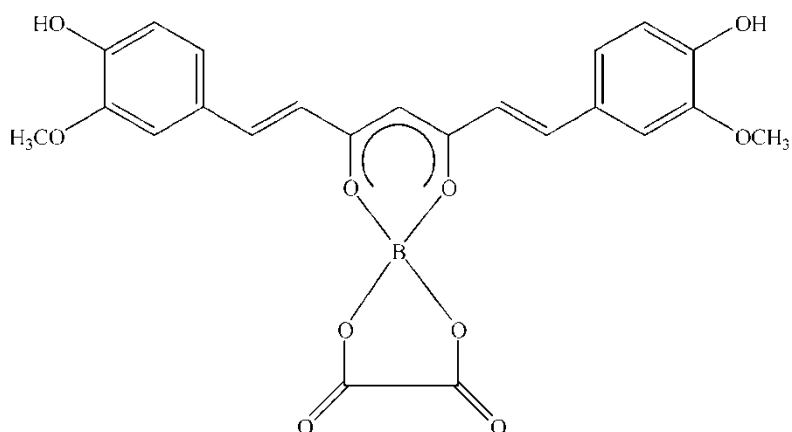


**Figure 2.9:** Structure of rubrocurcumin. One curcumin molecule is replaced with an oxalate in rosocyanine to form rubrocurcumin (Uppström, 1968).



### 2.8.2 Carminic acid

The reaction of carminic acid and boric acid in a concentrated sulphuric acid gives a blue complex. Carminic acid, which is a conjugated anthraquinone, is the cause of the blue colour. Carminic acid owes its application to some extent to broad optical concentration limits, comparatively few interferences and low reagent blanks. Spectrophotometric determinations were performed on samples in a sulphuric acid-acetic acid medium (Boltz and Howell, 1978). Absorbance was recorded at 300 nm, a wavelength at which the carminic acid method is most sensitive.

The diverse materials from which boron has been determined include rocks, water, and plants and biological matter. The carminic acid method has also been used for boron determination in titanium, molybdenum and in aluminium-uranium alloys (Boltz and Howell, 1978). The carminic acid method suffers from the use of strong sulphuric acid, 95% (17.8 M), which is used to prepare boron standards.

### 2.8.3 Quinalizarin

The reaction of boric acid and quinalizarin results in a blue 1:1 complex. This reaction occurs preferably in concentrated sulphuric acid medium. Quinalizarin, an intensely coloured reactant, has an absorbance maximum that partly covers that of boron-quinalizarin complex. Quinalizarin and its boron complex exhibit greatest absorbance disparities around 610 nm in sulphuric acid. The use of different concentrations of quinalizarin and changes in the procedure result in inconsistent sensitivities of the method. The utilisation of an acetic acid-sulphuric acid medium increases the sensitivity by approximately ten times as much (Boltz and Howell, 1978).

The quinalizarin method, like the carminic acid method, employs very strong sulphuric acid in the range 91 to 93% (17.8 M). This limits the use of this method for routine analysis.

#### **2.8.4 1,1'-dianthrimide**

The reaction of boric acid with 1,1'-dianthrimide, an aminoanthraquinone, in concentrated sulphuric acid results in a 1:1 blue complex (Boltz and Howell, 1978). The other name for 1,1'-dianthramide is 1,1'-iminodianthraquinone. Maximum colour development is achieved by heating the reaction mixture. The optimum heating temperature for the reaction mixture is 80 °C for 4.5 h. 1,1'-dianthrimide exhibits low absorbance in the wavelength measurement range of 1–10 µg boron. This determination method enjoys wide application for boron in different materials, which include soil, plants, low-alloy steels, titanium alloys and aluminium (Boltz and Howell, 1978).

#### **2.8.5 Methylene blue-tetrafluoroborate**

Separation of traces of boron from various materials was achieved by extraction of methylene blue-tetrafluoroborate complex with dichloroethane. Further studies confirmed the wide application of this method. The materials from which boron was determined include steel, tin, zirconium and rocks. To circumvent contamination, polyethylene and Teflon® ware must be used.

Total conversion of boric acid to tetrafluoroborate is the most important step in this method. Complete conversion of 1 M of boric acid can be achieved. This is a somewhat slow reaction, which requires about 2 h for complete conversion of 1 M of boric acid. The reaction is slower in less acidic solutions. The extraction time and acidity are important for making sure that methylene blue exists as a cation (Boltz and Howell, 1978).

There are various analytical techniques and methods for the determination of extracted boron. However, the separation or extraction of boron is by no means easy and neither is its quantification. Most of the analytical methods involving the formation of complexes are tedious and time-consuming. They also suffer from different interferences. Inductively coupled plasma (ICP) sources, e.g. ICP-mass spectrometry and ICP-optical emission spectrometry, compare favourably with the analytical method. Plasma sources are not only reliable, but also do not suffer from interferences (Sah and Brown, 1997).

The solvent extraction technique is the method of choice among other boron removal methods.

## 2.9 BORON USES

Boron is utilised in filaments and semiconductors for specialised aerospace applications. It is also used as a semiconductor in electrical applications (Jemmis and Balakrishnarajan, 2001). Non-crystalline boron is used in flame or bright light, which gives rise to the colour green. It is also used in flares to illuminate a target (Daintith, 2008). Borates can be utilised as fire retardants (Woods, 1994, Gross et al., 2008).

The high thermal shock resistance of borosilicate glass is attributed to boron oxide,  $B_2O_3$ . Boron oxide lowers the expansion coefficient of the glass, thereby increasing its thermal shock resistance (Woods, 1994). The mechanical stability and chemical endurance of fibreglass are greatly increased by the addition of boric oxide (Woods, 1994). Boron finds application in abrasives as a cutting and polishing material (Jemmis and Balakrishnarajan, 2001). Borates are used in welding rods owing to their outstanding ability to solubilise metal oxides (Woods, 1994).

Hardenability is a measure of a material's capacity to be hardened or made resilient by thermal treatment. Boron is a very strong alloying element for steels. It enhances the hardenability of steels when added in small amounts owing to its own hardening property. Boron is normally added to steels in the composition range of 0.0005 to 0.003%. It is efficacious at lower carbon contents. Minute amounts of boron have a significant effect on the hardenability and tensile strength of steel (Yamane et al., 2001, Coedo et al., 1993). However, high boron concentration may have a damaging effect on the strength of steels due to grain-boundary precipitation (Yurioka, 2001, Fu et al., 2008).

High strength, toughness and field weldability are outstanding properties exhibited by boron-bearing low-carbon bainitic steels. Bainite is a phase that exists in the microstructure of steel after heat treatment. Boron steels have found wide application in engineering, the manufacturing of oil pipes and sea platforms. Cu-B low-carbon bainitic

steels are resistant to oxidation and have been broadly employed in the building of bridges and war vessels (Wang and He, 2002).

Borax, a mined boron-containing mineral, has been used as a cleaning agent and an additive in laundry (Gross et al., 2008). Additive-formulated borax products have cleaning capability, as in household bleach. Borax improves water softness by tying up calcium ions (Woods, 1994). The United States is one of the two major sources of boron ores. Table 2.5 gives the approximate usage of these ores in the US.

**Table 2.5:** Estimated use of boron minerals and chemicals in the US (Woods, 1994).

Use	Percentage
Glass and ceramics:	
Insulation fibreglass	28
Textile fibreglass	12
Glass	9
Enamels and glazes	3
Detergents and bleaches	12
Alloys and metals	6
Fire retardants	5
Agriculture	4
Adhesives	2
Other chemicals	19

In agriculture, borates are utilised as fertilisers to correct the lack of minute amounts of boron in certain plants (Woods, 1994, Boncukcuoğlu et al., 2004). One application of boron that is also important is its use in insect powders (Boncukcuoğlu et al., 2004). Boron has an effect on a large number of biological functions that are seemingly unrelated (Bolaños et al., 2004).

It has been suggested that boron supplement may be effective in the treatment of painful, swelling of joints in the body. Boron is also thought to increase the hardness of the bones and prevent abnormal loss of bony tissue (Burguera et al., 2001). However, the role

played by boron in biochemical activities in humans and animals is still not clear (Sah and Brown, 1997). The permissible limit for boron in drinking water, according to the World Health Organization (WHO), is 0.5 g/ml (Xu and Jiang, 2008).

Boron has been proposed as a means for the storage and transportation for solar energy (Abu-Hamed et al., 2007).

A moderator that contains  $^{10}\text{B}$  can be used to control the reactivity in a nuclear reactor that uses controlled nuclear fission to generate energy. The moderator is any material in the nuclear reactor that slows down fast moving neutrons to thermal ones.  $^{10}\text{B}$  is also utilised in the form of boron carbide as a shutdown rod (Garton, 1957, Muetterties, 1967, Thangavel et al., 2006, Daintith, 2008).

It was not until 1936, only four years after the discovery of neutron, that the plan to fighting the deadly tumours was conceived (Plešek, 1992). This was the same year Locher suggested the binary nuclear reaction for potential cancer therapy, otherwise known as boron neutron capture therapy, BNCT (Barth et al., 1990, Hawthorne, 1991).

$^{10}\text{B}$  is used in BNCT owing to its high neutron capture cross section, 3837 barns (Barth et al., 1990, Hawthorne, 1991, Plešek, 1992). BNCT is a new cancer treatment method which uses  $^{10}\text{B}$  and neutron radiation to kill cancerous cells without affecting adjacent healthy cells (Sah and Brown, 1997). Low energy (0.025 eV) or thermal neutrons irradiation of  $^{10}\text{B}$ , a stable boron isotope, gives helium nuclei ( $\alpha$ -particles) and  $^7\text{Li}$ .

## CHAPTER THREE: EXPERIMENTAL

### 3.1 MATERIALS

Sasol supplied the medium-temperature gasifier pitch for this research. High-purity organic solvents were purchased from Merck. Boron model compounds were purchased from Sigma Aldrich and were of high purity.

### 3.2 ASH DETERMINATION

The ash content of pitch indicates the amount of undesirable residue. Ash is undesirable as it does not contribute to the carbon yield and can be unfavourable for processing and carbon performance. In general, ash comprises the metal oxides originally present in the pitch. MTP samples of 20 to 25 g were transferred to pre-weighed platinum crucibles and heated to 550 °C in a muffle furnace. The samples were maintained at this temperature for 4 h. After cooling, the ash content was determined as follows:

$$\text{Ash, wt \%} = \left( \frac{A - B}{C} \right) \times 100 \quad (3.1)$$

where

A = weight of crucible and residue after ashing

B = weight of empty crucible

C = weight of MTP before ashing

### 3.3 SOLUBILITY EXPERIMENTS

All solubility tests were performed at ambient temperature. These tests were performed to determine good and poor solvents for the MTP. A good solvent is one that would dissolve MTP completely without traces of precipitates, whereas a poor solvent leaves a lump of pitch on the filter paper. One gram of MTP was dissolved in 10 ml of an organic solvent in a test tube. The test tubes were sealed airtight with stoppers to prevent evaporation of solvents and were stored at ambient temperature for 2 days for complete dissolution of

the MTP. During the two-day period, the solutions were shaken sporadically to improve dissolution of the MTP. The shaking was performed carefully to prevent the solution from touching the stopper.

The second solubility test was also performed at ambient temperature to quantify the extract and residue and to determine the solubility limit of MTP. The solubility of MTP was determined by transferring pitch samples (5, 10, 20, 30, 40 and 50 g) into 500 ml propylene bottles to which 100 ml of organic solvent was added. The bottles were tightly closed and intermittently shaken for a period of 30 days.

Thereafter the extract was filtered under vacuum with a pre-weighed Whatman<sup>®</sup> filter paper No. 2. This filter paper can retain particles of 8  $\mu\text{m}$  and larger. The extract is the filtrate that passes through the filter paper and the residue is the solid matter remaining on the filter paper. The residue, i.e. the insoluble fraction, was dried in an oven at 75 °C until a constant mass was obtained.

### **3.4 EXTRACT RECOVERY**

The filtrate was transferred into a round-bottom flask and placed in a rotary evaporator, shown in Figure 3.1. Due to their relatively low boiling points, methanol (64.7 °C) and tetrahydrofuran (66 °C) were recovered under reduced pressure. The dissolved MTP was transferred into a 250 ml round-bottom flask, immersed in a hot-water bath and rotated. The rotation continuously wets the warm walls of the flask where evaporation is rapid and prevents bumping. This method also prevents the loss of solvent. For quinoline, N,N-dimethylformamide (DMF) and pyridine, due to their high boiling points, the extract was recovered by placing a round-bottom flask on the heating mantle in an extraction hood until all the solvent had evaporated.

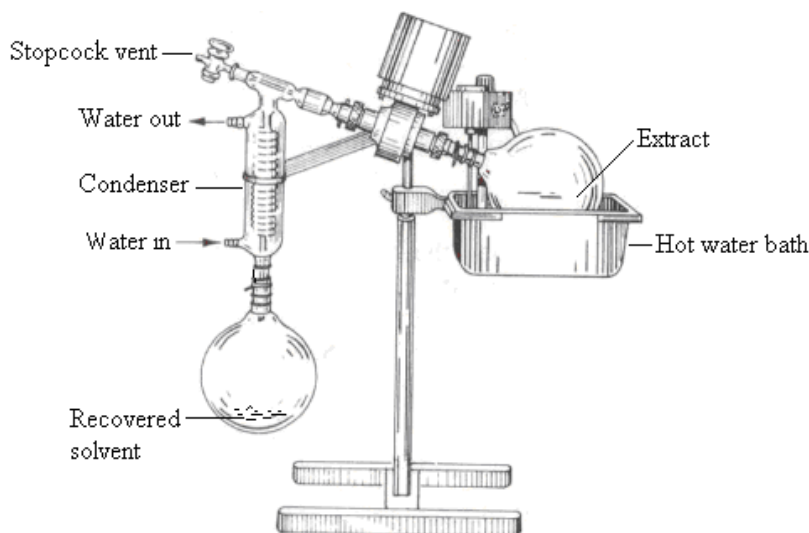


**Figure 3.1:** Schematic diagram of a typical rotary evaporator for extract and solvent recovery (Pasto and Johnson, 1989).

After it had been cooled to ambient temperature, the flask was weighed and the extract was determined by difference. This method may result in overheating, thereby decomposing the sample. This is a challenge, especially for solvents with high boiling points. The extraction yield for MTP was determined on a dry, ash-free basis using the following equation:

$$\text{Extraction yield (\%)} = \frac{1 - \left( \frac{\text{mass of residue (g)}}{\text{mass of MTP (g)}} \right)}{1 - \left( \frac{\text{Ash (\%)}}{100} \right)} \times 100 \quad (3.2)$$

### 3.5 DOPING OF BORON MODEL COMPOUNDS

Boron-doped pitch samples, 0.1 wt % B, were prepared by adding boron model compounds to molten pitch. The required mass of MTP was weighed and transferred into a round-bottom flask. The corresponding boron model compound was weighed and added into the flask. The mixture was heated gently on a heating mantle and swirled when the pitch started to melt. The continuous swirling facilitated dissolution of the boron model compound in the pitch. The mixture was black and viscous and that made it difficult to



see whether the model compound had completely melted or not. As a measure of dissolution, the mixture was heated until small particles of boron model compound were no longer visible. This was used as an indication that the model compound had fully dissolved or dispersed in the pitch. After a uniform mixture had been formed, the flask was removed from the heating mantle and cooled to ambient temperature. Boron acid model compounds with their physical properties is shown in Figure 3.2.

### **3.5.1 Simulated boron removal**

Methanol was added into the flask containing the pitch samples spiked with 1 000 ppm B in the ratio 1 g pitch:1.5638 g methanol. The mixture was heated under reflux for 2 h to remove the laced boron from the pitch. After 2 h of reflux extraction, the mixture was cooled to ambient temperature. Two phases formed upon cooling, namely the top phase, a methanol-rich phase, and a bottom phase, which was an insoluble pitch. The methanol-rich layer was decanted into an empty PTFE flask and gently heated on a heating mantle to liberate methanol and the extract was recovered. The pitch-rich fraction remained inside the flask. This fraction was removed with dichloromethane because of its viscosity. The dissolved pitch phase was then transferred into a PTFE beaker and heated on a heating mantle to release the low-boiling dichloromethane. The boron content of both the methanol-rich and pitch-rich phases was determined by inductively coupled plasma optical emission spectroscopy (ICP-OES) based on the American standard ASTM D 5158-02.

MTP samples without boron model compounds were extracted with methanol to quantify the extract. This was achieved by dissolving the pitch in methanol with the same extraction ratio used for boron removal. The mixture was refluxed for 2 h and allowed to cool to ambient temperature after the reflux period. The methanol-rich phase was transferred into a pre-weighed 100 ml Petri dish and put in the oven set at 80 °C. The purpose was to liberate methanol and retain the extract. The dish was removed from the oven and allowed to cool to room temperature. It was then weighed until a constant mass was obtained and the percentage extracted was calculated.

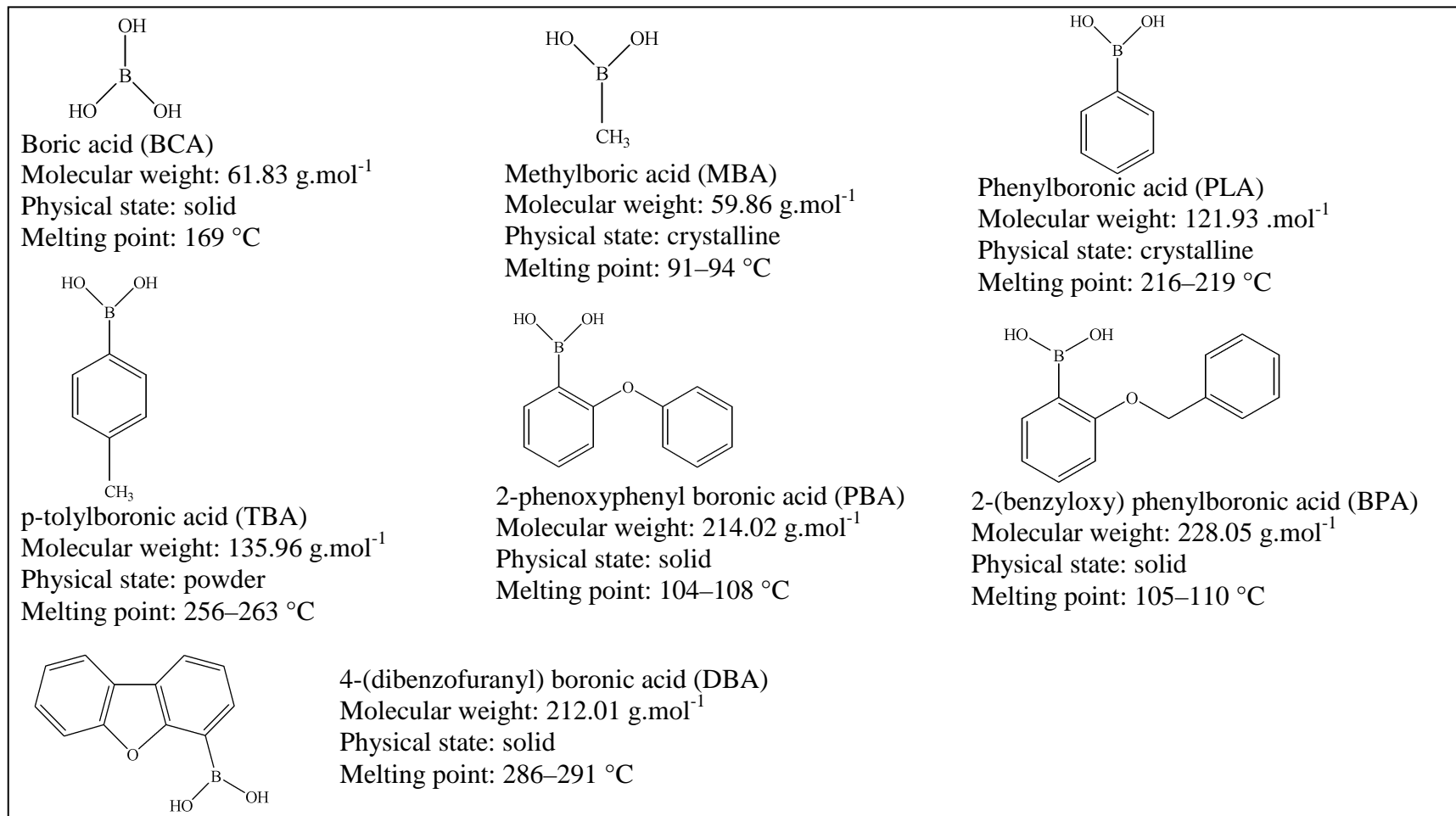


**Figure 3.2:** Boron model compounds used for doping medium-temperature gasifier pitch (MTP). MTP was spiked with each model compound to prepare 0.1 wt % (1000 ppm) B samples.

### **3.5.2 Boron determination**

Combustion of organic samples prior to analysis results in the loss of an analyte due to volatilisation and precipitation (Hausler, 1987). Direct determination of trace elements with ICP-OES in organic samples presents an alternative to conventional ashing methods for organic samples. Trace elements have been determined in petroleum samples using the xylene solvent system (Hausler, 1987). Boron content was determined directly from methanol fraction samples and the pitch-rich residues with ICP-OES compatible with organic samples. The analysis was based on ASTM D 5158-02. This method compares favourably with the conventional ashing of organic samples prior to analysis as it circumvents the loss of boron.

## **3.6 STRUCTURAL ANALYSIS**

Pitches comprise thousands of different compounds with various molecular weight ranges and are important carbon precursors. Understanding the structure and properties of MTP would help to optimise its conversion to advanced carbon materials. Several techniques were used to study the properties of this material.

### **3.6.1 Elemental analysis**

The elemental compositions of MTP and its fractions were acquired on a Carlo Erba NA 1500 C/N/S Analyzer. This instrument is equipped with two quartz furnaces for oxidation and reduction respectively. The oven of this instrument is fitted with a chromatographic column for the separation of N<sub>2</sub>, CO<sub>2</sub>, SO<sub>2</sub> and H<sub>2</sub>O vapour. The instrument has a thermal conductivity detector. The carrier gas, helium, which is also used as a reference, is used for sample purging prior to analysis. The instrument was modified by removing water vapour to determine the hydrogen content.

### **3.6.2 Infrared spectroscopy**

IR spectra were collected with a PerkinElmer Spectrum RX IFT-IR System equipped with MIRacle™ attenuated total reflectance (ATR) for spectrometers by PIKE Technologies. The spectra were recorded in the range 4000–600 cm<sup>-1</sup>, averaging 32 scans

for each sample. The instrument's resolution was  $2.0 \text{ cm}^{-1}$  with intervals of  $1.0 \text{ cm}^{-1}$ . Aromaticity indices ( $I_{\text{ar}}$ ) were estimated from the spectra using the following equation (Guillén et al., 1992):

$$I_{\text{ar}} = \frac{\text{Abs}_{3050}}{\text{Abs}_{3050} + \text{Abs}_{2920}} \quad (3.4)$$

### 3.6.3 Nuclear magnetic resonance

Solid-state NMR spectra were collected on a Varian VNMRS 500 MHz two-channel spectrometer. Four mm zirconia rotors and a 4 mm Chemagnetics™ T3 HX MAS probe were used. All cross-polarisation (CP) spectra were recorded at ambient temperature with proton decoupling, a  $2.9 \mu\text{s}$   $90^\circ$  pulse, and a recycle delay time of 2 s. The power parameters were optimised for the Hartmann-Hahn match; the radiofrequency fields were  $\gamma_{\text{C}}B_{\text{IC}} = \gamma_{\text{H}}B_{\text{IH}} \approx 56 \text{ kHz}$ . The contact time for cross-polarisation was 1.0 ms after optimisation with a variable contact time experiment. One-pulse spectra were recorded at ambient temperature with proton decoupling, a  $2.9 \mu\text{s}$   $90^\circ$  pulse, and a recycle delay time of 80 s. The free induction decay had 1 787 complex points, Fourier transformed with 20 Hz line broadening. Magic-angle spinning (MAS) was performed at 9 kHz. Adamantane was used as an external chemical shift standard where the downfield peak was referenced to 38.3 ppm.

### 3.6.4 MALDI-TOF

The average molecular weight distributions of pitch samples and their extracts can be estimated reliably by mass spectrometer. Matrix-assisted laser desorption/ionisation time of flight (MALDI-TOF) is a technique used for determining the molecular weight distribution of many complex organic compounds (Domin et al., 1998). Sample preparation in MALDI-TOF involves mixing the analyte with an organic matrix compound such as dihydrobenzoic acid (Watson and Sparkman, 2007). Edwards et al. (2003) used 7,7,8,8-tetracyanoquinodimethane (TCNQ) as an organic matrix compound and obtained consistent mass spectra for insoluble pitch fractions.

The sample is prepared for analysis by mixing the analyte and matrix compound in the molar ratio 1:5 000. It is worth mentioning, however, that this ratio depends on the kind of matrix compound used and is not fixed. The matrix separates analyte molecules by dilution, thereby preventing analyte-analyte molecular or ionic interactions during ionisation. The main function of the matrix is to protect the analyte from radiation damage by absorbing radiation (Edwards et al., 2003). The organic matrix compound is generally chosen on the basis of the solubility properties of the analyte. The high energy density illuminates the sample matrix, thus transforming the analyte into neutral molecules and ions (Watson and Sparkman, 2007).

An Applied Biosystems Voyager-DE STR MALDI-TOF spectrometer was used in reflector mode. The target plate was positively charged and set to 20.0 kV. The mass range was scanned from 20 to 1 000 m/z. Each sample was dissolved in 1 ml chloroform and spotted onto the plate without the matrix. After spotting, the samples were allowed to dry before they were analysed.  $\alpha$ -cyano-a-4-hydroxycinnamic acid was used as the matrix. Important parameters used in this study included a delayed extraction mode, an extraction delay time of 500 ns, manual acquisition control and a grid voltage of 70%.

### 3.6.5 GC-MS

Some of the compounds found in coal tar pitches cause cancer and are capable of inducing mutation. Analysis of the concentration of PAHs in the carbon artefact precursors is therefore of importance. The gas chromatograph-mass spectrometer (GC-MS) is a powerful instrument for the determination of PAHs. Gas chromatography (GC) is a separation technique and a mass spectrometer (MS) is a quantification instrument. The concentration of PAHs in the MTP was determined using a GC-MS.

The pitch sample was dissolved in dichloromethane and the chromatograms were collected on an Agilent 6890 HP GC and an Agilent 5973 MS. The GC was fitted with a Restek Rxi-5ms column 30 m in length, with an internal diameter of 0.25 mm and with 0.25  $\mu$ m film thickness. The injector temperature was set at 320 °C with an injection volume of one  $\mu$ l. Helium was used as the carrier gas with a flow rate of 1.2 ml.min<sup>-1</sup>.

The mass spectrometer was set at 230 °C transfer temperature with the electron energy set at 70 eV.

### **3.7 THERMAL ANALYSIS**

Thermal analysis monitors some physical changes, e.g. mass loss, softening point and glass transition temperature, in a sample subjected to a controlled temperature under specified conditions. Various techniques are used to study these and other properties: thermomechanical analysis, thermogravimetric analysis, differential thermogravimetry, differential scanning calorimetry, etc.

#### **3.7.1 Softening point**

The softening point of pitch is the temperature at which the pitch attains a particular degree of softening under controlled analysis conditions. In general, pitches with a higher average molecular weight distribution exhibit higher softening points. A TMA Q400 V22.1 analyser was used to analyse the softening point of MTP and its fractions. A penetration probe with 0.05 N was used for softening point measurements. The measurements were performed by placing the probe on the sample and bringing the thermocouple probe closer to the sample. The softening point was measured under 50 ml.min<sup>-1</sup> nitrogen flow and at a 2 °C.min<sup>-1</sup> heating rate. A cylindrical furnace surrounded the quartz tube, sample and probe during heating.

#### **3.7.2 Thermogravimetric analysis**

The measurement of a sample's mass against its temperature or time under a controlled temperature programme in a given environment is referred to as thermogravimetry (TG) (Fifield and Kealey, 1995). Chemical processes such as thermal degradation, physical degradation (evaporation) and loss of volatiles can also be studied with this technique. The results can be presented graphically as a thermogravimetric curve. The mass percentage is plotted on the ordinate, decreasing downwards and the temperature or time on the abscissa increasing from left to right. TG also provides the thermal stabilities of various kinds of material, thus giving their qualitative 'fingerprint'. This also helps in identifying different samples.

### 3.7.3 Differential thermogravimetry

The first derivative of a TG curve is called differential thermogravimetry (DTG). The resultant curve is plotted on the ordinate as a differential mass with respect to time and temperature on the abscissa. The total change in mass of the sample is proportional to the area of the peak. Thermal analysis was performed using a Mettler Toledo A851 TGA/SDTA thermal analyser. About 20 mg samples were placed in open 70  $\mu\text{l}$  aluminium pans. The temperature was scanned from 25 to 1000  $^{\circ}\text{C}$  at 10  $^{\circ}\text{C}\cdot\text{min}^{-1}$  with nitrogen flowing at 50  $\text{ml}\cdot\text{min}^{-1}$ .

## CHAPTER FOUR: RESULTS AND DISCUSSION

### 4.1 SOLUBILITY

The solubility test results are presented in Figures, 4.1, 4.2 and 4.3. The results show that MTP is highly soluble in tetrahydrofuran, quinoline, toluene, dimethylformamide and xylene. A ring of uniform colour formed on the filter paper indicates the extent of solubility of MTP in a given solvent. Solvents that give a ring of constant colour can be regarded as powerful solvents for MTP. However, the faint yellow that appeared as ‘solutions’ of hexane and formamide (not shown here) were applied was due to solvent only and not to the mixture of MTP and solvent. MTP was virtually insoluble in these solvents. The behaviour of MTP in hexane is peculiar because hexane has been widely used in the fractionation of pitches (Menéndez et al., 2000).

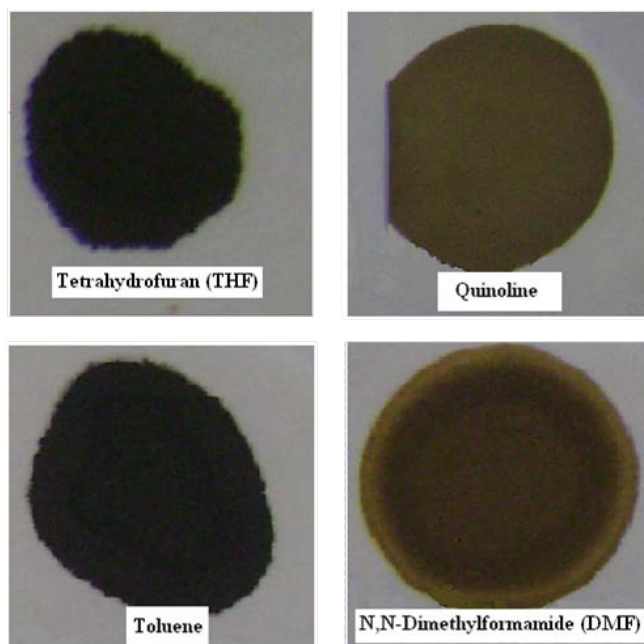


**Figure 4.1:** Solubility test results showing some powerful solvents for MTP. Experiments were conducted at ambient temperature with 1 g MTP in 10 ml of solvent for 2 days.



A black spot at the centre of the circle indicates the presence of a precipitate or residue. In Figure 4.2, dark spots for acetone and dimethyl sulphoxide at the centre are clearly visible. They indicate incomplete dissolution of MTP, under the given conditions of 1 g of MTP per 10 ml of solvent, in those solvents. However, it is worth mentioning that the degree of extraction depends on various factors such as temperature and solvent:MTP ratio. These results are only valid for the given conditions under which the solvent extraction tests were performed.

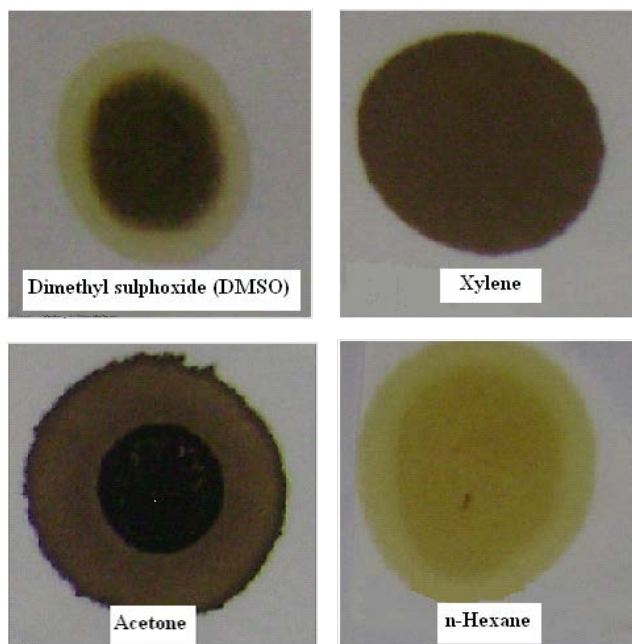


**Figure 4.2:** Solubility tests showing some good and poor solvents for MTP. Experiments were conducted at ambient temperature with 1 g of MTP in 10 ml of solvent for 2 days.

Figure 4.3 shows that the degree of MTP extraction was constant for DMF, quinoline tetrahydrofuran (THF) and pyridine. This suggests that the solubility limit of MTP in these solvents was not reached and it is expected to exceed 40 g/100 ml solvent. MTP was practically insoluble in formamide. This behaviour was also observed by Blanco and Guillén (1991) when determining the solubility of a coal tar pitch in different solvents. The degree of MTP extraction in methanol declined with increasing ratio of MTP to methanol. Saturation was also reached when the ratio of MTP to methanol was increased.

Consequently, the selection of methanol as an organic solvent for removing boron was based on the following reasons:

- (i) MTP has limited solubility in methanol.
- (ii) There is an expected interaction between boron with the alcohol –OH functional group. Hydroxyl compounds have been used to remove boron from fresh waters (Ayers et al., 1981).

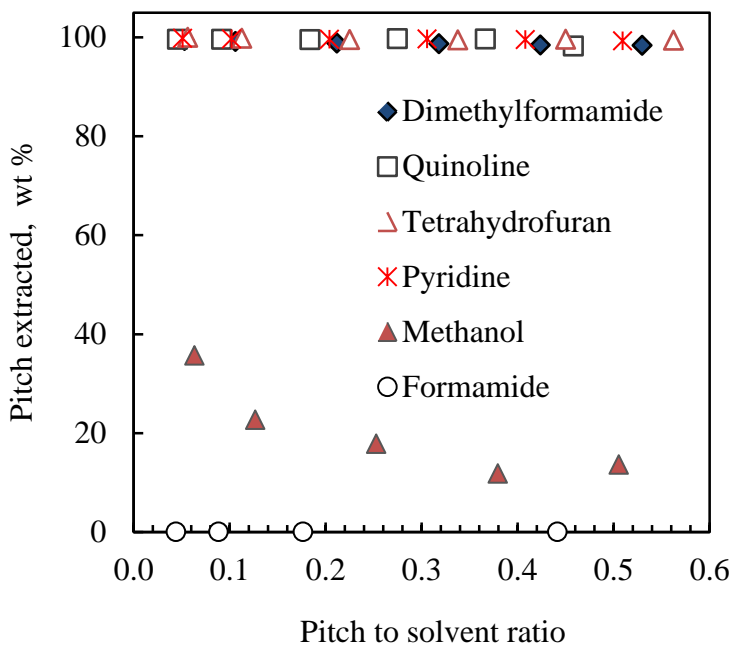


**Figure 4.3:** Effect of pitch:solvent ratio on the extraction yield. Experiments were performed at ambient temperature for 30 days with sporadic shaking applied to the mixtures during this period.

## 4.2 DETERMINATION OF BORON

Figure 4.4 shows that methanol extraction effectively reduced the boron content to values ranging from 133 ppm methyl boronic acid (MBA) and 542 ppm phenylboronic acid (PLA). The former compound and boric acid were removed most effectively and this is attributed to the formation of highly volatile methyl esters. It is also likely that some of the other boron compounds were stripped from the pitch residues as volatile boronic acid esters when the methanol was distilled off. This justifies the decision to define the apparent boron partition coefficients based on the boron content of the recovered pitch residues.

4-(dibenzofuranyl) boronic acid (DBA), 2-phenoxyphenyl boronic acid (PBA), p-tolylboronic acid (TBA) and phenylboronic acid (PLA) were the most retained in the residues after methanol extraction. Over 500 ppm of PBA, TBA and PLA were retained in the pitch residues following methanol extraction. The results suggest that these model compounds, which have a high degree of aromaticity compared with methyl boric acid (MBA) and boric acid (BCA), are difficult to remove with methanol extraction. The high boron percentage in the extracts of samples spiked with PBA and PLA could not be accounted for.

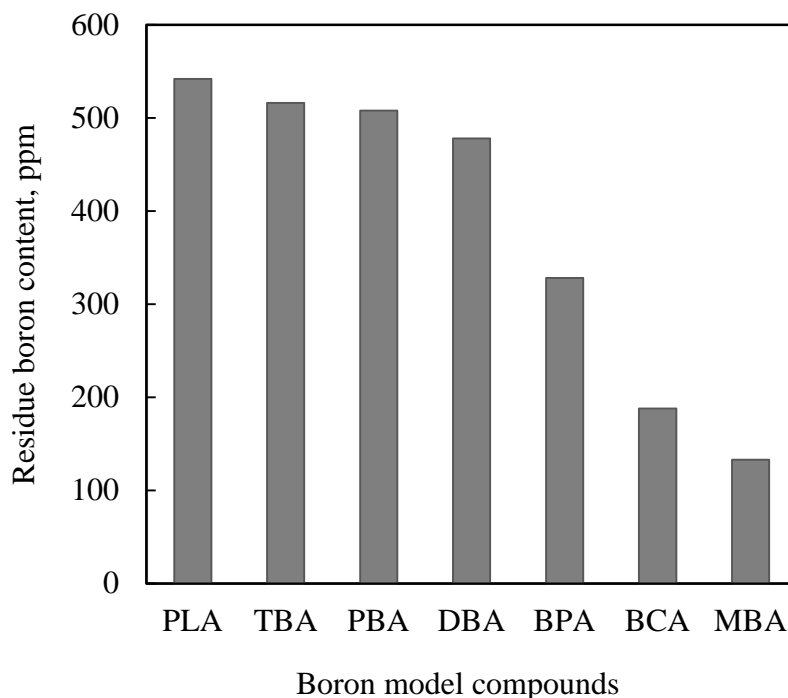


**Figure 4.4:** Boron content of extract and residue of MTP initially spiked with 1000 ppm B after 2 h of reflux extraction with methanol.

### 4.3 STRUCTURAL ANALYSIS

Different techniques revealed important structural information on MTP and its fractions. The results of all the techniques used to characterise MTP and its fractions are presented in the following subsections.

#### 4.3.1 Elemental analysis

Elemental analyses of MTP and its fractions are presented in Table 4.1. The data show that MTP comprises mainly carbon and hydrogen. The oxygen content is relatively higher than that of nitrogen and sulphur. This was also observed by Sima and colleagues (2003). They attributed the high oxygen content to the high concentration of phenols that was found in MTP.

The aromaticity index, determined according to Equation 3.4 (section 3.6.2), reflects the aromaticity of the pitch and its fractions. The aromaticity increases with the use of a powerful solvent for MTP. The benzene- and toluene-insoluble fractions showed high

aromaticity and low sulphur content as compared with the parent pitch and the methanol-insoluble fraction. A high sulphur content is not desired because it causes puffing during the heat treatment of pitch materials. The ash content of MTP was 0.09 wt %.

**Table 4.1:** TMA softening point and elemental analysis of MTP and its fractions.

Sample	SI	SP	I <sub>Ar</sub>	C	H	N	S	O	C/H
Parent pitch (MTP)	nd	38.50	34	85.32	6.39	1.95	0.51	5.83	1.12
Methanol insolubles	45.83	59.61	41	87.07	6.34	1.82	0.53	4.24	1.15
Toluene insolubles	3.00	nd	44	84.14	5.43	2.91	0.33	7.19	1.30
Benzene insolubles	3.33	nd	45	83.23	4.96	2.83	0.31	8.67	1.40

SI = solvent insoluble, wt %; nd = not determined; SP = softening point, °C; I<sub>Ar</sub> = aromaticity index (FTIR), C = carbon content wt %; H = hydrogen content, wt %; N = nitrogen content, wt %; S = sulphur content, wt %; O = oxygen content (by difference), wt %; C/H atom ratio.

### 4.3.2 ATR-infrared spectroscopy

Attenuated total reflectance (ATR) spectra of MTP and its soluble and insoluble fractions in various organic solvents were obtained. Functional and structural information on pitches and their fractions can be obtained by studying the difference in the intensities of their characteristic bands (Guillén et al., 1992).

Figures 4.5, 4.6 and 4.7 show the infrared spectra of MTP and its soluble and insoluble components in methanol, toluene and benzene. These spectra are similar except for their intensities in some characteristic absorption regions. The existence of aromatic rings is generally determined by C–H stretching which occurs above 3000 cm<sup>-1</sup>. This is characteristically exhibited by weak to moderate bands as compared with aliphatic C–H stretching.

The spectra of MTP and its methanol-soluble and -insoluble fractions are presented in Figure 4.5. The spectrum of the methanol-soluble fraction is similar to that of MTP. The spectrum of the methanol-insoluble fractions differs somewhat from the other two spectra. With IR spectroscopy, it is possible to differentiate MTP from its fractions. The main difference lies in the intensities of characteristic C–H bands.

A band around  $2920\text{ cm}^{-1}$ , due to aliphatic C–H stretching, is less pronounced in the methanol-insoluble fraction. A band around  $3050\text{ cm}^{-1}$ , which is due to aromatic C–H stretching, is intense for the methanol-insoluble fraction. This indicates that methanol dissolves largely alkyl groups (side chains) attached to the aromatic network. This is in agreement with the aromaticity indices of MTP (34%), and the methanol-soluble (27%) and methanol-insoluble (41%) fractions. The aromaticity indices were determined from the spectra following a method described by Guillén et al (1992).

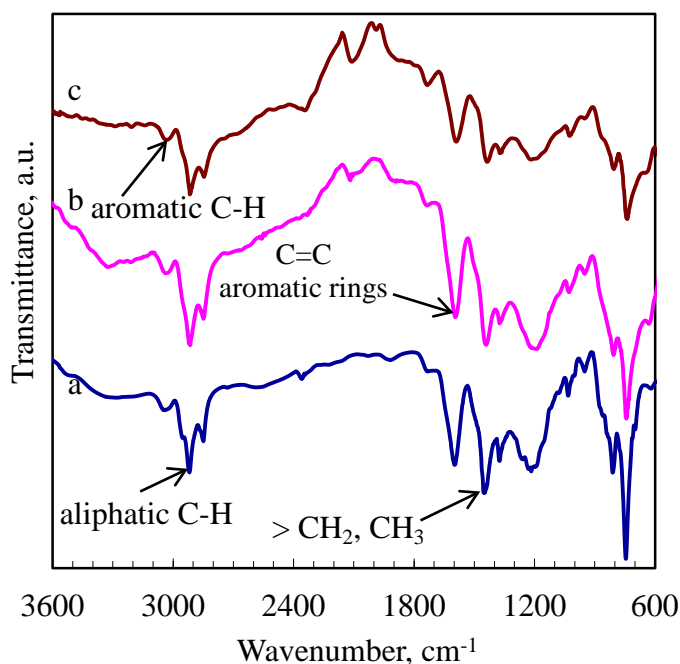


**Figure 4.5:** ATR spectra of (a) MTP, and its (b) methanol-soluble and (c) methanol-insoluble fractions. MTP fractions were prepared by refluxing 2 g of MTP in 100 ml of methanol for 30 min.

The bands around  $3050\text{ cm}^{-1}$  for both the toluene- and benzene-insoluble fractions are more intense than in their corresponding soluble fractions. The bands at  $2920\text{ cm}^{-1}$ , due to aliphatic C–H stretching, are not pronounced. This suggests that the toluene- and benzene-insoluble fractions have higher aromatic hydrogen content than their corresponding soluble fractions.

The band around  $3050\text{ cm}^{-1}$  for both the toluene- and benzene-insoluble fractions (Figures 4.6 and 4.7) are more intense than in their corresponding soluble fractions. The aliphatic C–H stretching bands around  $2920\text{ cm}^{-1}$  are not pronounced. This indicates that benzene and toluene dissolved substantially the low molecular weight species and larger aromatic components of the MTP. This results in the insoluble fractions from both solvents having higher aromatic contents than their corresponding soluble fractions.

A band around  $730\text{ cm}^{-1}$  is related to four or five adjacent methylene ( $-\text{CH}_2-$ ) groups in an aliphatic chain (Colthup, 1950). This band is more intense in the parent pitch and its soluble fractions compared with the corresponding insoluble fractions. This corroborates the point made earlier that aromatic C–H stretching was stronger in the insoluble fractions than in the soluble fractions.

Another observation made is that benzene and toluene dissolve more aliphatic compounds than methanol. The solubility data indicated that methanol was a poor solvent for MTP and this is agreement with the observations made here with ATR infrared spectroscopy.

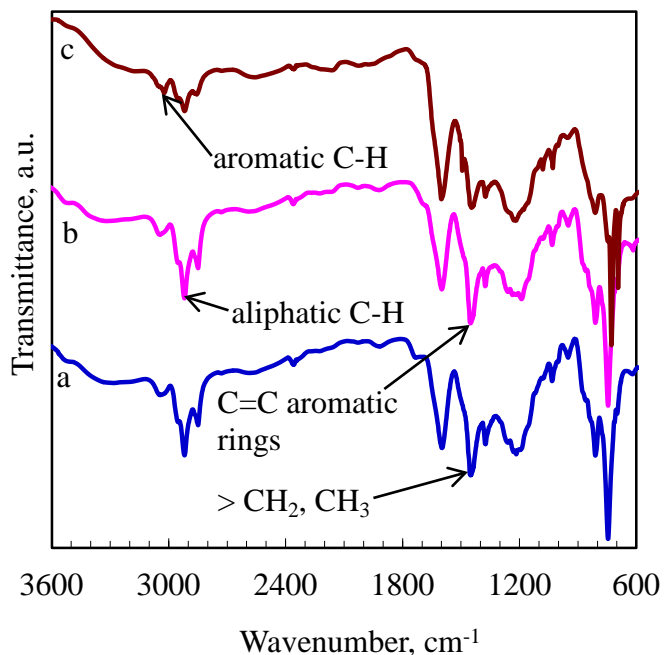


**Figure 4.6:** ATR spectra of (a) MTP, and (b) its toluene-soluble and (c) toluene-insoluble fractions. MTP fractions were prepared by refluxing 2 g of MTP in 100 ml of toluene for 30 min.

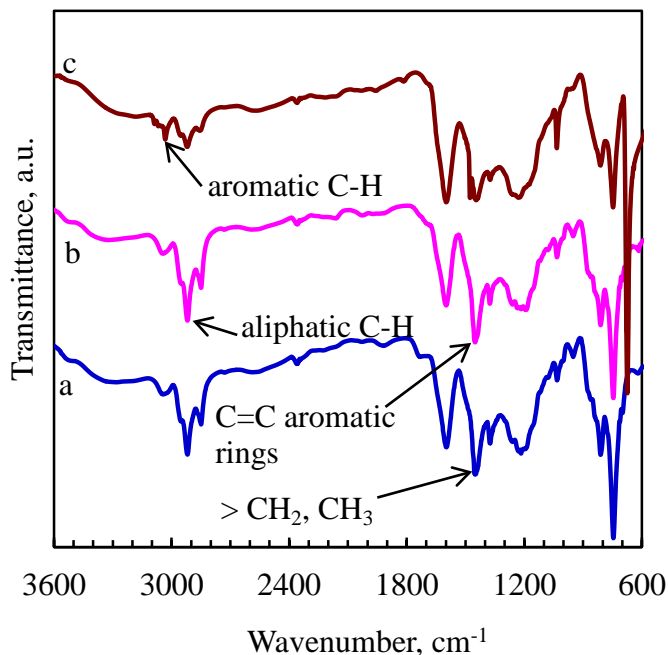


**Figure 4.7:** ATR spectra of (a) MTP and (b) its benzene-soluble and (c) -insoluble fractions. MTP fractions were prepared by refluxing 2 g of MTP in 100 ml of benzene for 30 min.



The bands in the region 2912 to 2844  $\text{cm}^{-1}$  are due to the distribution of aliphatic hydrogens ( $-\text{CH}_2-$ ) (Alcañiz-Monge et al., 2001). Analysis of the bands in this region shows that the insoluble fractions of all three solvents contain less linear aliphatic structures compared with their corresponding soluble fractions and the parent pitch (Coates, 2000). The bands in the regions 2912 to 2844  $\text{cm}^{-1}$  and 1435 to 1364  $\text{cm}^{-1}$  indicate that aliphatic hydrogens are present largely as  $-\text{CH}_2-$  structures. These bands are relatively weak in the insoluble components of the three solvents. This is in agreement with the observation made that these solvents (methanol, benzene and toluene) dissolve largely the aliphatic structures of the parent pitch. A band around 1375  $\text{cm}^{-1}$  shows the presence of cyclic structures (Alcañiz-Monge et al., 2001).

The benzene-insoluble fractions have higher aromatic hydrogen content (2800–2980  $\text{cm}^{-1}$ ) than the parent pitch. This is an indication that large planar aromatic molecules are present in the insoluble fractions. The same can be said for the toluene insoluble fractions, whose spectrum resembles that of the benzene-insoluble fractions in the range 3800–1600  $\text{cm}^{-1}$ . These large molecules are important for the formation of mesophase (Lim and Lee, 1991). The intensity of the bands for aliphatic hydrogen drops significantly in both the benzene- and toluene-insoluble fractions (2800–2980  $\text{cm}^{-1}$ ).

### 4.3.3 Nuclear magnetic resonance

The solid-state  $^{13}\text{C}$  NMR spectra of MTP and its soluble and insoluble fractions were obtained. Long instrument time is needed to scan just one sample. Long relaxation time is also required to allow the sample to release energy before a new scan is started. The quantitative data presented in Table 4.2 show that the toluene- and benzene-insoluble fractions have high aromaticity compared with MTP and their corresponding soluble fractions.

All the spectra for MTP and its fractions have an asymmetric peak in the region of the 127 ppm shift. This peak is indicative of the presence of aromatic carbons (Pasto and Johnson, 1989). The peak in the region of the 0–50 ppm shift indicates significant presence of aliphatic carbons. Magic-angle spinning (MAS) is not sufficient to eliminate

the anisotropic effect of dipolar interactions and magnetic shielding. This results in spinning sidebands occurring in the frequency distances of 9 kHz.

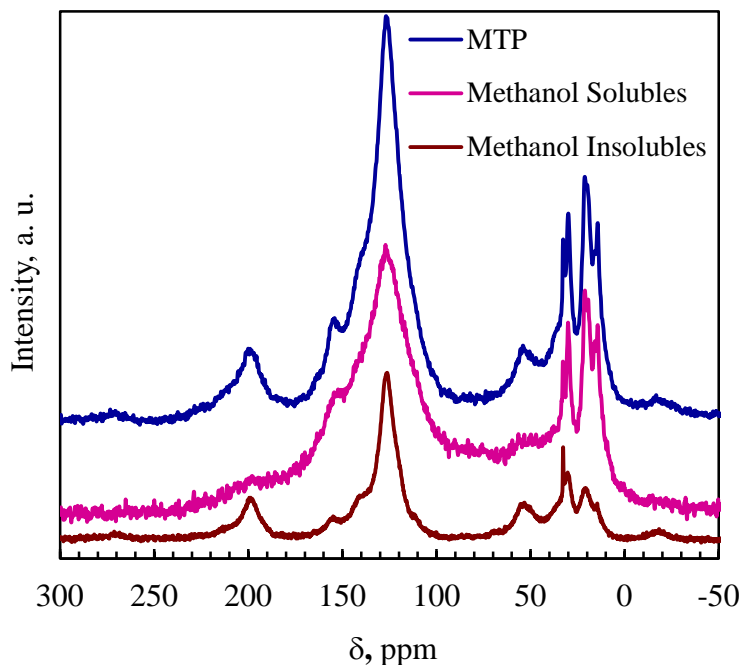


**Figure 4.8:** Solid-state  $^{13}\text{C}$  NMR CP MAS spectra of MTP and its methanol-soluble and -insoluble fractions.

All the spectra but one for the methanol soluble and insoluble fractions showed a double aromatic peak in the range 120–160 ppm. The aliphatic carbon peaks in Figures 4.8 to 4.10 for the MTP fractions insoluble in the three solvents are less pronounced compared with MTP. This suggests that the corresponding solvent removed a high concentration of aliphatic compounds. These results are consistent with those obtained with IR and elemental analysis, i.e. treatment of MTP with organic solvents increases its aromaticity by removing light molecular weight compounds.

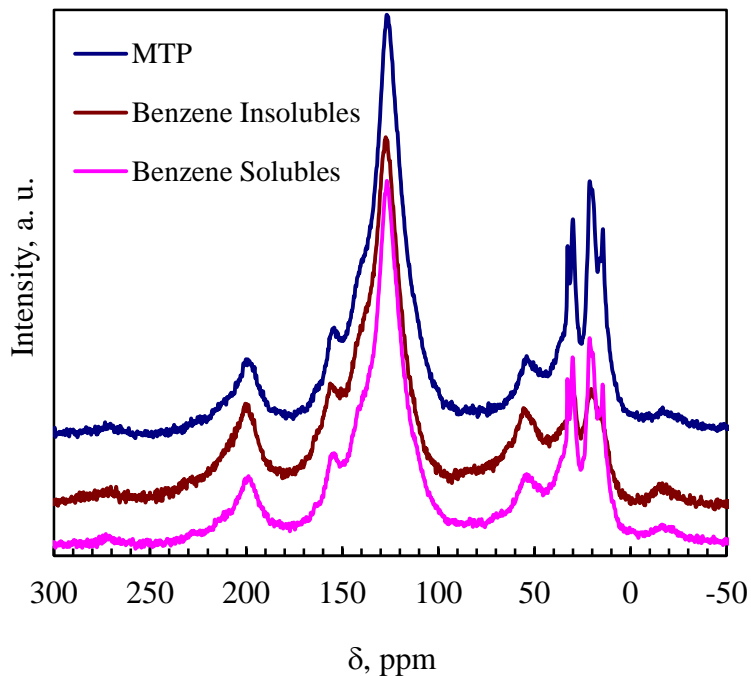


**Figure 4.9:** Solid-state  $^{13}\text{C}$  NMR CP MAS spectra of MTP and its benzene-soluble and -insoluble fractions.

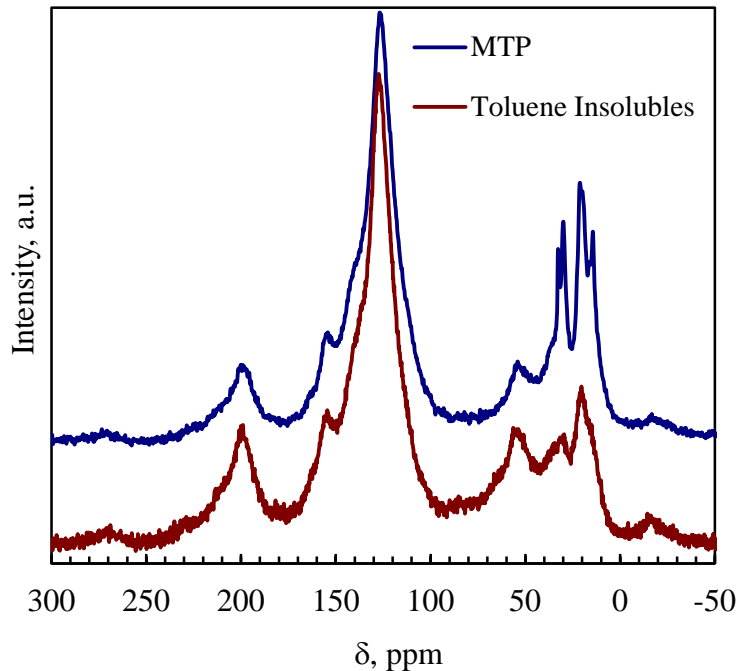


**Figure 4.10:** Solid-state  $^{13}\text{C}$  NMR CP MAS spectra of MTP and its toluene-insoluble fractions.

A peak at 200 ppm is due to the spinning sidebands of aromatic carbons. A broad, spinning sideband at 55 ppm is attributed to the aliphatic carbons. The spinning sidebands of the aromatic peak may be covering or overlying the signals of other carbon species. The spinning sideband at 200 ppm may be covering the carbonyl signals and that at 55 ppm may be partially overlying the CH<sub>2</sub>-carbon signal and covering the carboxylate signals.

The difficulty in interpreting the spectra could be solved by comparing the CP-MAS spectra with CP-MAS total side band suppression (TOSS) spectra. In the latter technique, the spinning sidebands of the aromatic carbons are suppressed (Mokoena et al., 2008b). Using this technique, the carboxylate signals were identified and subtracted from the integral of the spinning sideband at 200 ppm of the CP-MAS spectra. A pure aliphatic carbon signal partially covered by the spinning sideband at 55 ppm was measured as well.

The determination of the aromaticity factor and the ratio of aliphatic to aromatic carbons were determined by the CP-MAS method, which is non-quantitative. Consequently, further interpretation may be restricted to identifying and comparing trends, in contrast to the interpretational work with absolute values.

Figure 4.11 shows that both the benzene-insoluble (BI) and toluene-insoluble (TI) fractions have higher aromaticity fractions. The results indicate that BI and TI comprise a higher amount of large aromatic molecular compounds. However, the amount of large compounds in these fractions relative to raw MTP is very small. The aromaticity fractions of BI and TI indicate that benzene and toluene are strong solvents for MTP. The aromaticity fraction of MTP is the same as that of the benzene solubles.

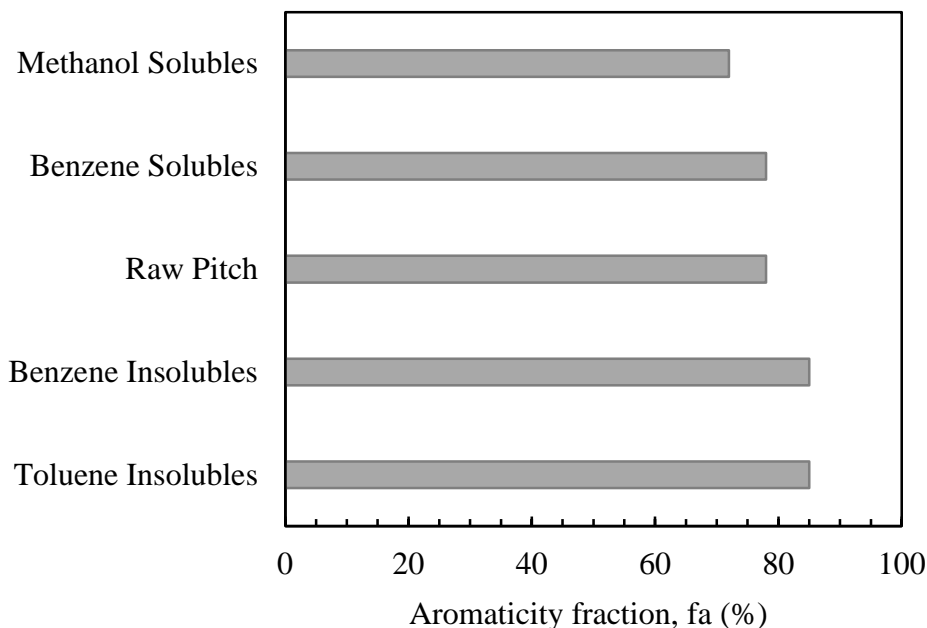


**Figure 4.11:**  $^{13}\text{C}$  NMR data for MTP and its fractions. All fractions were determined by refluxing 2 g of MTP in 100 ml of solvent for 30 min.

#### 4.3.4 Molecular mass distributions

Figure 4.12 shows the MALDI mass spectrum of the MTP. The results show that the isotropic MTP consists predominantly of low molecular weight compounds as compared with other commercial pitches. The MALDI mass spectra of the MTP and its solvent-soluble and -insoluble fractions were studied at an ion accelerating voltage of 20 kV. These MALDI mass spectra were collected without the matrix and showed a broad peak of ion intensity in the range 200–400 m/z.

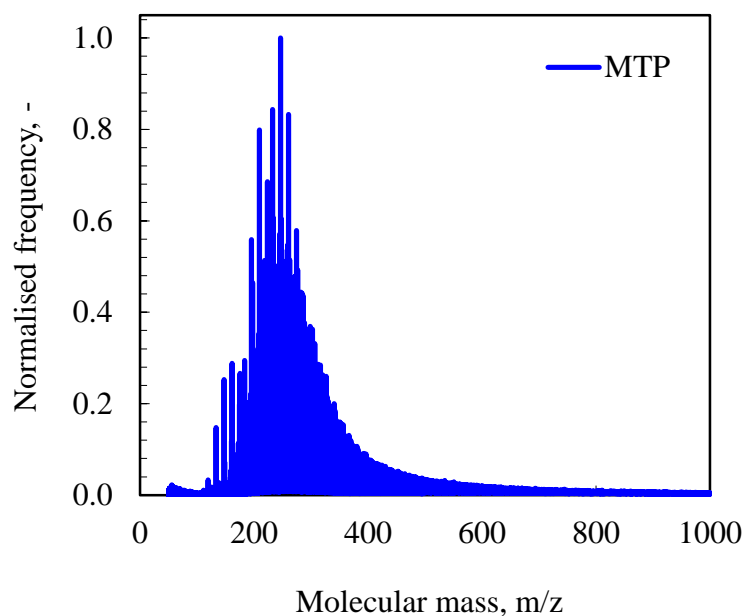


**Figure 4.12:** MALDI mass spectrum of the parent pitch, MTP. The plot shows that MTP is composed largely of compounds in the low molecular mass range.

All the spectra, except for the methanol-soluble fractions, show a continuum of peaks from 400 to 1 000 m/z. However, this continuum is less intense as the peaks in the range 200–400 m/z.

The MALDI mass spectra of MTP, and the solvent-soluble and -insoluble fractions are presented in Figures 4.12 to 4.17. All these spectra show maximum ion intensity in the range 200–400 m/z. This confirms the observation made that these fractions as well as the parent pitch, MTP, comprise largely low molecular weight species. Most of the compounds are found in the low molecular mass region, 190–388 m/z, and only a few are in the high molecular mass region, 388–645 m/z.

These results are consistent with those obtained from TMA and TGA. The softening point is a function of the molecular mass distribution. The TMA results showed that MTP had a very low softening point, 38.5 °C, which suggests a high presence of low molecular weight species. The TGA results also showed that MTP and its solvent-soluble and -insoluble fractions had a low carbon yield.

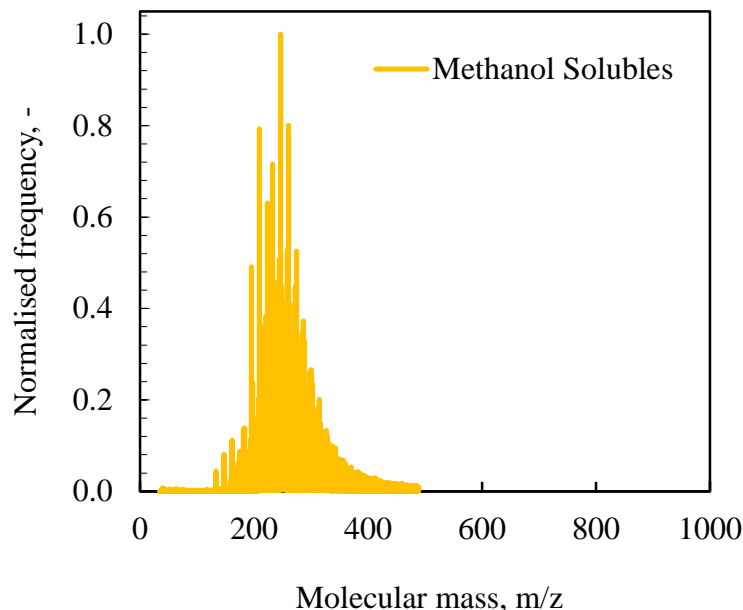


**Figure 4.13:** MALDI mass spectra of the methanol-soluble fractions showing their molecular mass distribution.

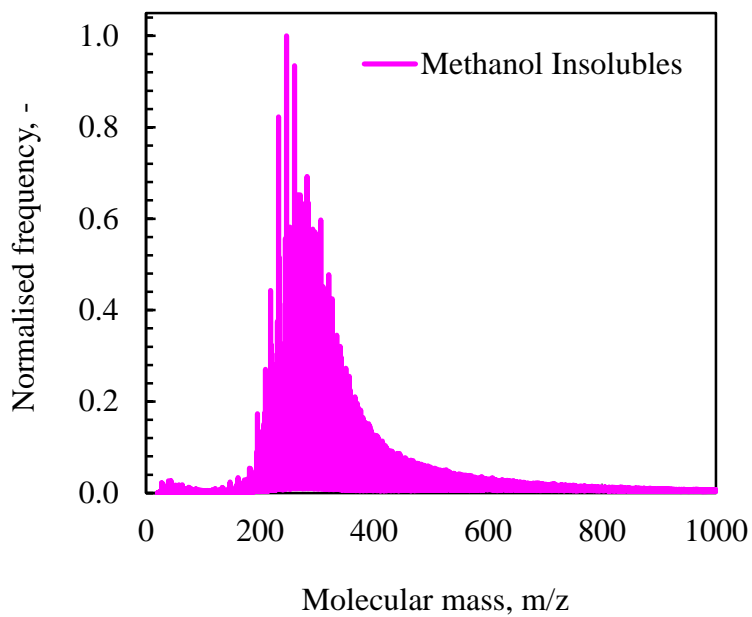


**Figure 4.14:** MALDI mass spectra of the methanol-insoluble fractions showing their molecular mass distribution.



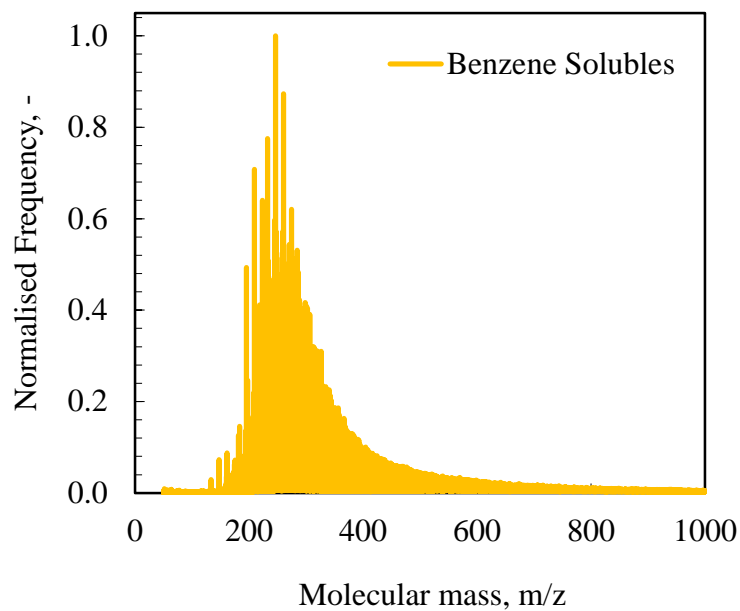


**Figure 4.15:** MALDI mass spectra of the benzene-soluble fractions showing their molecular mass distribution.

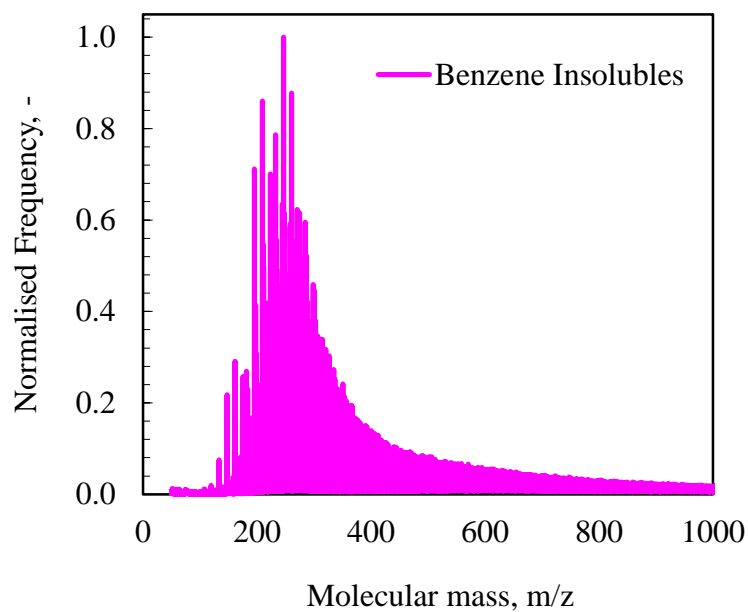


**Figure 4.16:** MALDI mass spectra of the benzene-insoluble fractions showing their molecular mass distribution.

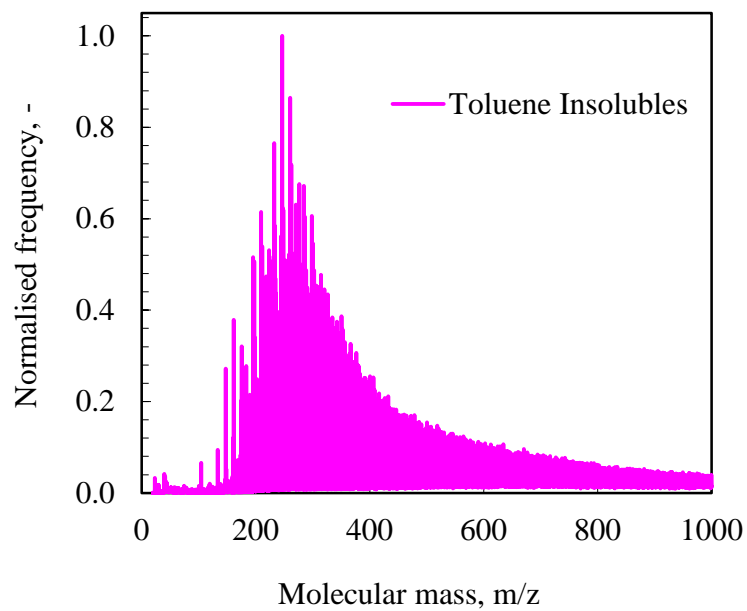


**Figure 4.17:** MALDI mass spectra of the toluene-insoluble fractions showing their molecular mass distribution.

The weight average molecular mass ( $M_w$ ), number average molecular mass ( $M_n$ ) and polydispersity index (PDI) of the parent pitch and its soluble and insoluble fractions are given in Table 4.2. The PDI is defined as the ratio of the weight average to the number average molar masses ( $PDI = M_w:M_n$ ). It provides a measure of the width of the molar mass distribution. The PDI of the parent pitch and methanol-insoluble and benzene-soluble fractions were similar, equalling 1.23, 1.22 and 1.21 respectively. Both the toluene- and benzene-insoluble fractions featured a broader molar mass distribution compared with the methanol-soluble pitch fraction, which has a narrower molar mass distribution.

**Table 4.2:** Important MALDI features of MTP and its fractions.

<b>Sample Identity</b>	<b>Mn</b>	<b>Mw</b>	<b>PDI</b>
Methanol solubles	272	288	1.06
Raw pitch (MTP)	327	403	1.23
Benzene solubles	358	434	1.21
Methanol insolubles	359	437	1.22
Toluene insolubles	432	543	1.26
Benzene insolubles	420	553	1.32

Mn is defined as the number average molecular mass and Mw is the weight average molecular mass. PDI is the polydispersity index defined as the ratio,  $M_w:M_n$

The results in Table 4.2 show that both toluene and benzene are powerful solvents that dissolve large compounds. Consequently, these solvents could not be used for extraction purposes in this study. Methanol was the ideal solvent for extraction because it dissolved largely low molecular mass compounds, leaving behind large molecular compounds.

#### 4.3.5 Evaluation of PAHs by GC-MS

Table 4.3 shows the results for the estimation of polycyclic aromatic hydrocarbons (PAHs) in the parent pitch, MTP, and its methanol-soluble and -insoluble fractions. The methanol-soluble and -insoluble fractions were prepared by refluxing MTP and methanol in the ratio 1 g MTP:1.5638 g methanol for 30 min. Determination of the PAH content of commercial pitches is becoming increasingly important. PAHs are known to be carcinogenic and efforts to produce pitches with low toxicity are continuing (Alvarez et al., 2009).

The concentrations of PAHs were determined from GC-MS and the results are given in mg/g. The benzo(a)pyrene equivalent, a measure of toxicity of all PAHs combined, was estimated by multiplying the concentration of each PAH by the corresponding relative potency factor (McHenry and Saver, 1996) and summing them.

The results show that the PAH concentration of both MTP and the methanol-soluble fraction are relatively higher than that of the methanol-insoluble fraction. However, the benzo(a)pyrene equivalent, abbreviated to B(a)P equivalent, for the methanol-insoluble fraction is slightly higher than those of MTP and the methanol-soluble fraction. Looking at individual concentrations of PAH, the results show that the methanol-insoluble fraction has no naphthalene and acenaphthene compared with MTP and the methanol-soluble fraction. There was no acenaphthylene in all three samples.

The decline in the concentration of eight PAHs seen in the methanol-insoluble fraction is attributable to the action of methanol on the MTP. Methanol is not a powerful solvent for MTP. It dissolves low molecular weight compounds. This is also supported by the high concentrations of three high molecular weight ( $\geq 276.34$ ) PAHs in the methanol-insoluble fraction. Overall, the results suggest that treatment of MTP with methanol prior to processing does not only result in higher carbon yield but also in low PAH concentration.

**Table 4.3:** Estimation of PAHs and benzo[a]pyrene equivalent, B(a)P, in MTP and its methanol-soluble (MS) and -insoluble (MI) fractions.

<b>Compound</b>	<b>PQL</b>	<b>RPF</b>	<b>MTP</b>	<b>MS</b>	<b>MI</b>
	<b>mg/g</b>		<b>mg/g</b>	<b>mg/g</b>	<b>mg/g</b>
Naphthalene	0.001	0.000	0.84	0.36	0.00*
Acenaphthylene	0.001	0.000	0.00	0.00	0.00
Acenaphthene	0.001	0.000	0.61	0.55	0.00*
Fluorene	0.001	0.000	4.50	4.80	0.08
Phenanthrene	0.001	0.000	12.00	13.00	0.56
Anthracene	0.001	0.000	4.10	5.20	0.46
Fluoranthene	0.001	0.034	6.10	7.30	1.60
Pyrene	0.001	0.000	5.30	6.60	1.60
Benzo[a]anthracene	0.001	0.033	3.60	4.70	1.60
Chrysene	0.001	0.260	3.90	5.00	1.90
Benzo[b]+[k]fluoranthene	0.001	0.100	4.60	5.60	3.80
Benzo[a]pyrene	0.001	1.000	1.80	2.20	1.80
Indeno[1,2,3-cd]pyrene	0.001	0.100	1.10	0.99	1.60
Dibenzo[a,h]anthracene	0.001	1.400	0.46	0.48	0.60
Benzo[g,h,i]pyrene	0.001	1.000	1.90	1.60	3.30
PAH content, mg/g			50.81	58.38	18.90
B(a)P equivalent, mg/g			6.25	6.83	7.08

PQL is the practical quantification limit and RPF is the relative potency factor.

\*These polycyclic aromatic hydrocarbons are relatively soluble in methanol.

## 4.4 THERMOMECHANICAL ANALYSIS

Like many coal tar pitches of different origins, MTP does not exhibit a sharp melting point. The results for the determination of the softening points of MTP and its methanol-insoluble fractions are given in Figures 4.18 and 4.19 respectively. These show that MTP has a low softening point, 39 °C, as compared with the methanol-insoluble fraction, 59 °C. The softening points of the benzene- and toluene-insoluble fractions proved difficult to measure.

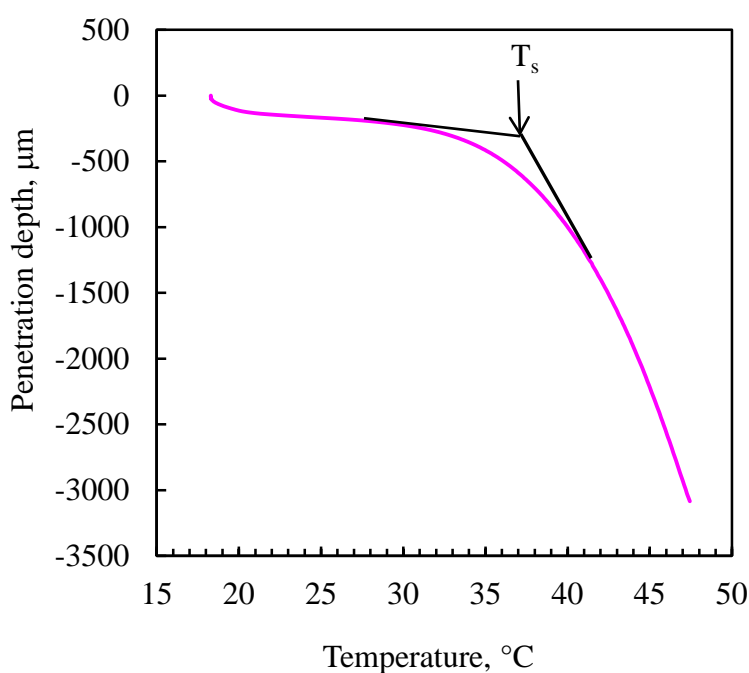


**Figure 4.18:** TMA curve showing determination of the softening point ( $T_s$ ) of raw MTP.

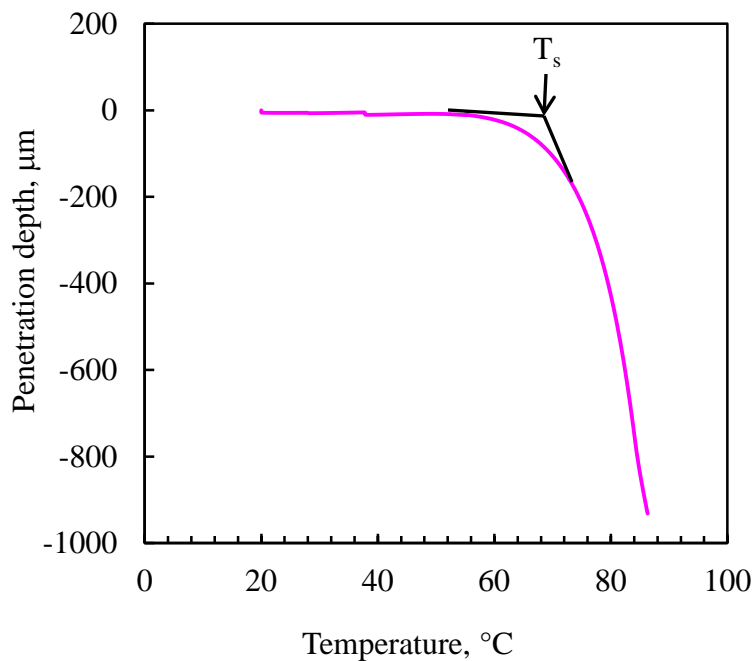


**Figure 4.19:** TMA curve showing determination of the softening point ( $T_s$ ) of the methanol-insoluble pitch fraction.

The results suggest that MTP and its methanol-soluble fraction can be used as an impregnator or binder because of their low softening points. Pitches with high softening points, i.e. 100 °C or greater, are the best candidates for forming cokes.

## 4.5 THERMOGRAVIMETRIC ANALYSIS

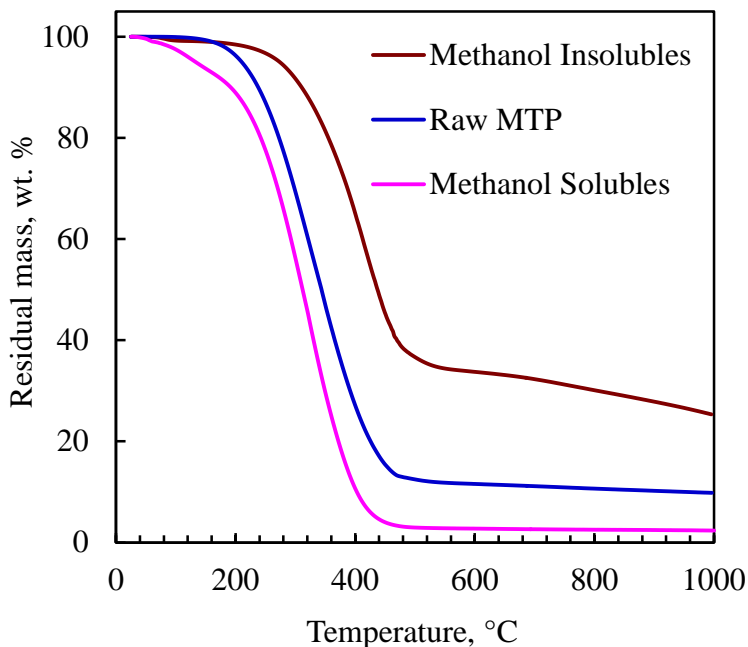


**Figure 4.20:** TGA curves of raw MTP and its methanol-soluble and -insoluble fractions in N<sub>2</sub>.

Figure 4.20 shows that MTP and its methanol-soluble and -insoluble fractions undergo weight loss in a single step, covering an interval from 40 to 450 °C. The initial weight loss in the methanol-insoluble fraction around 96 °C is attributed to the loss of moisture and traces of methanol. The methanol-insoluble fraction exhibits a relatively higher onset temperature and is thus thermally stable compared with raw MTP and the methanol-soluble fraction.

Methanol insolubles have a higher carbon yield (25 wt %) than raw MTP (9.8 wt %) and the methanol-soluble fractions (2.4 wt %). The low carbon yield of the methanol-soluble fraction suggests that methanol dissolved mostly low molecular weight species. The results also indicate that dissolving MTP in organic solvents prior to thermal treatment increases its thermal stability and the carbon yield.



Figures 4.21 and 4.22 show that both the benzene- and toluene-insoluble fractions have higher carbon yields than the parent pitch and their corresponding soluble fractions. The results also show that the benzene- and toluene-insoluble fractions have higher thermal stabilities than the parent pitch and their corresponding soluble fractions. This behaviour was also observed when methanol was used.

There was little volatilisation for both the benzene- and toluene-insoluble fractions below 330 °C, whereas a great deal of weight loss occurred in the temperature range 330 to 500 °C. These solvents remove low molecular weight species that are not important for mesophase formation. The removal of these species by the solvents also results in high carbon yield.

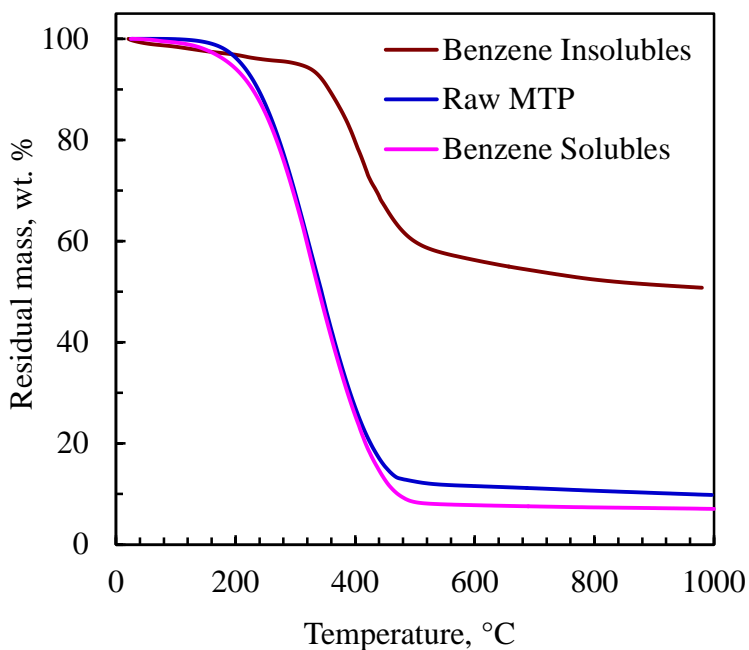


**Figure 4.21:** TGA curves of raw MTP and its benzene-soluble and -insoluble fractions in N<sub>2</sub>.

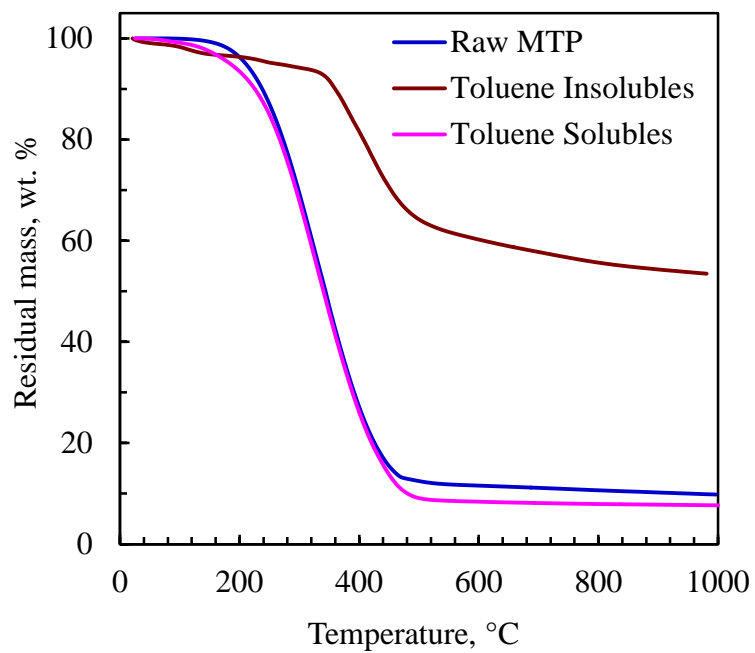


**Figure 4.22:** TGA curves of MTP and its toluene-soluble and -insoluble fractions in  $N_2$ .

Figure 4.23 shows that raw MTP is thermally stable and has a higher carbon yield than the toluene-, benzene- and methanol-soluble fractions. Toluene and benzene dissolve virtually all the MTP and thus they are powerful solvents for MTP. Figure 4.23 also shows that the benzene- and toluene-soluble fractions have low carbon yields compared with MTP. This indicates that MTP comprises largely low molecular weight species and fewer PAHs (Sima et al., 2003).

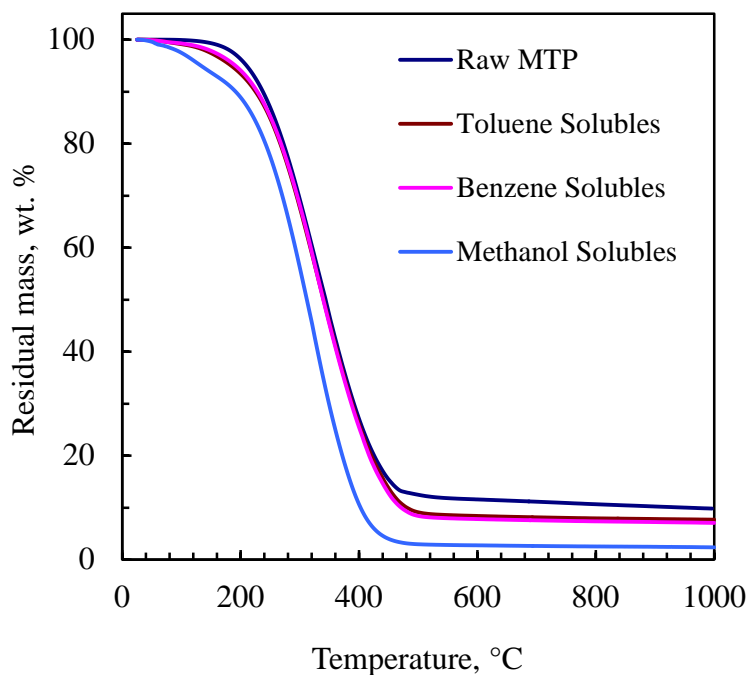


**Figure 4.23:** TGA curves showing all soluble fractions having low carbon yield compared with MTP in N<sub>2</sub>.

Figure 4.24 shows the DTG curves of MTP and its insoluble fractions. The presence of low molecular weight species is also indicated in the DTG curves. MTP loses most of its weight at a lower temperature of 317 °C compared with the methanol-insoluble fraction whose weight loss band is around 424 °C. The toluene-insoluble fraction shows a broad band around 400 °C due to the distillation of light compounds. The band around 100 °C is attributed to the loss of moisture.

There are two bands for the benzene-insoluble fraction around 400 and 440 °C, which are related to the distillation of light compounds. The results suggest that treating MTP with solvents prior to heat treatment may increase its thermal stability and carbon yield.

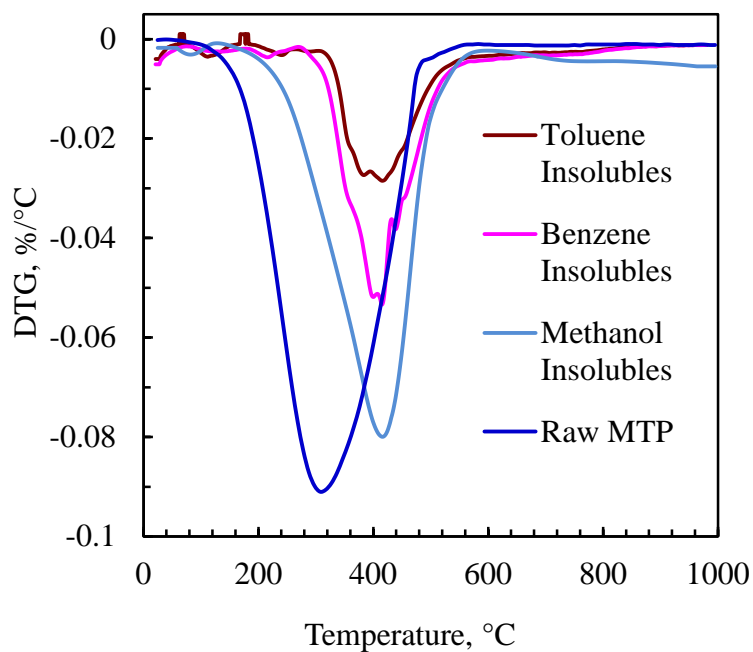


**Figure 4.24:** DTG curves of MTP and its insoluble fractions in different organic solvents in N<sub>2</sub>.

## CHAPTER FIVE: CONCLUSIONS

Medium-temperature gasifier pitch (MTP) was virtually completely soluble in dimethylformamide, quinoline, tetrahydrofuran, pyridine, morpholine, benzene, toluene, xylene and acetone. It was almost insoluble in *n*-hexane and formamide. MTP was slightly soluble in methanol; methanol dissolved mostly low molecular mass compounds with an aliphatic character that are not important for graphitisation. The results showed that the solubility limit of MTP in methanol is about 40 g/l at ambient temperatures.

4-(dibenzofuranyl) boronic acid (DBA), 2-phenoxyphenyl boronic acid (PBA), *p*-tolylboronic acid (TBA) and phenylboronic acid were the most retained in the residues after methanol extraction. The residues ranged in decreasing order of boron content after methanol extraction following this trend: PLA>TBA>PBA>DBA>BPA>BCA>MBA. The results showed that methanol could be used to remove various boronic acid compounds from MTP.

MTP and its fractions, methanol, toluene and benzene insolubles comprise largely carbon and hydrogen. The sulphur content of the toluene and benzene insolubles was higher than that of MTP and its methanol-insoluble fractions. The C/H ratio of the fractions followed this trend: MTP<MIs<TI<BI.

Methanol, toluene and benzene insolubles are more aromatic than their corresponding soluble fractions. The aromaticity indices for the insoluble fractions followed the same trend as the C/H ratio. MTP has the same aromaticity index as the benzene solubles. This was expected because benzene is a powerful solvent for MTP and dissolved almost the whole of the MTP, leaving only small amounts of residue. The benzene and toluene insolubles are composed predominantly of larger molecular mass compounds. This is supported by their relatively high aromaticity indices compared with those of MTP and the methanol insolubles, which are equal.

MALDI analysis revealed that the average molecular weight distribution followed the same trend as that of the C/H ratios and the aromaticity indices. The results also showed that most of the compounds in all four samples are in the low molecular mass range. Furthermore, the MALDI analysis revealed that MTP is composed largely of low molecular mass compounds.

The methanol-insoluble fractions showed low PAH content compared with the methanol-soluble fractions and MTP. The B(a)P equivalent for the methanol insolubles was slightly higher than those of the methanol solubles and MTP were.

Thermomechanical analysis for the softening points showed that MTP has a low softening point. The methanol-insoluble fractions showed an improved softening point; this is attributed to the removal of low molecular mass compounds.

The benzene-, toluene- and methanol-insoluble fractions showed high thermal stability and better carbon yield than their corresponding soluble fractions. Methanol has the best carbon yield of all the soluble fractions. This suggests that the soluble fractions cannot be useful for further processing into advanced carbon materials.

## CHAPTER SIX: REFERENCES

- ABU-HAMED, T., KARNI, J. & EPSTEIN, M. (2007) The use of boron for thermochemical storage and distribution of solar energy. *Solar Energy*, 81, 93-101.
- ALCAÑIZ-MONGE, J., CARZORLA-AMORÓS, D. & LINARES-SOLANO, A. (2001) Characterisation of coal tar pitches by thermal analysis, infrared spectroscopy and solvent fractionation. *Fuel*, 80, 41-48.
- ALVAREZ, P., GRANDA, M., SUTIL, J., SANTAMARÍA, R., BLANCO, C., MENÉNDEZ, R., FERNÁNDEZ, J. J. & VINA, J. A. (2009) Preparation of Low Toxicity Pitches by Thermal Oxidative Condensation of Anthracene Oil. *Environmental Science & Technology* 43, 8126 - 8132.
- AYERS, P., DUDENEY, A. W. L. & KAHRAMAN, F. (1981) Solvent extraction of boron with 2-ethyl-1,3-hexanediol and 2-chloro-4-(1,1,3,3-tetramethylbutyl)-6-methylol-phenol. *J. inorg. nucl. Chem*, 43, 2097-2100.
- BALL, D. R. (1978) The influence of the type of quinoline insolubles on the quality of coal tar binder pitch. *Carbon*, 16, 205-209.
- BARTH, R. F., SOLOWAY, A. H. & FAIRCHILD, R. G. (1990) Boron Neutron Capture Therapy of Cancer. *Cancer Research*, 50, 1061-1070.
- BARTON, A. F. M. (1983) *CRC Handbook of Solubility Parameters and Other Cohesion Parameters* Boca Raton, CRC Press Inc.
- BLANCO, C., PRADA, V., SANTAMARÍA, R., BERMEJO, J. & MENÉNDEZ, R. (2002) Pyrolysis behaviour of mesophase and isotropic phases isolated from the same pitch. *Journal of Analytical and Applied Pyrolysis*, 63, 251-265.
- BLANCO, C. G. & GUILLÉN, M. D. (1991) Study of Relationships between Solvent Effectiveness in Coal Tar Pitch Extractions and Solvent Solubility Parameters *Ind. Eng. Chem. Res.*, 30, 1579-1582.
- BOLAÑOS, L., LUKASZEWSKI, K., BONILLA, I. & BLEVINS, D. (2004) Why boron? *Plant Physiology and Biochemistry*, 42, 907-912.

- BOLTZ, D. F. & HOWELL, J. A. (1978) *Colorimetric Determination of Nonmetals*, John Wiley & Sons, Inc.
- BONCUKCUOĞLU, R., YILMAZ, A. E., KOCAKERIM, M. M. & ÇOPUR, M. (2004) An empirical model for kinetics of boron removal from boron-containing wastewaters by ion exchange in a batch reactor. *Desalination*, 160, 159-166.
- BOURRAT, X. (2000) Structure in Carbons and Carbon Artifacts. IN MARSH, H. & RODRÍGUEZ-REINOSO, F. (Eds.) *Sciences of Carbon Materials*. Universidad de Alicante, Secretariado de Publicaciones.
- BROOKS, J. D. & TAYLOR, G. H. (1965) The formation of graphitising carbons from the liquid phase. *Carbon*, 3, 185-193.
- BURGUERA, M., BURGUERA, J. L., RONDÓN, C. & CARRERO, P. (2001) Determination of boron in blood, urine and bone by electrothermal atomic absorption spectrometry using zirconium and citric acid as modifiers. *Spectrochimica Acta Part B*, 56, 1845-1857.
- CARREIRA, P., MARTÍNEZ-ESCANDELL, M., JIMÉNEZ-MATEOS, J. M. & RODRÍGUEZ-REINOSO, F. (2003) Chemistry of the co-pyrolysis of an aromatic petroleum residue with a pyridine-borane complex. *Carbon*, 41, 549-561.
- COATES, J. (2000) Interpretation of Infrared Spectra, A Practical Approach. IN MEYERS, R. A. (Ed.) *Encyclopedia of Analytical Chemistry*. Chichester, John Wiley & Sons.
- COEDO, A. G., DORADO, T., ESCUDERO, E. & COBO, I. G. (1993) Boron Determination in Steels by Inductively Coupled Plasma Atomic Emission Spectrometry. Comparative Study of Spark Ablation and Pneumatic Nebulization Sampling Systems *Journal of Analytical Atomic Spectrometry*, 8, 827-831.
- COLTHUP, N. B. (1950) Spectra-Structure Correlations in the Infra-Red Region. *Journal of the Optical Society of America*, 40, 397-400.
- DAINTITH, J. (2008) *A Dictionary of Chemistry*. Sixth ed., Oxford Press.
- DOMIN, M., LI, S., LAZARO, M.-J., HEROD, A. A., LARSEN, J. W. & KANDIYOTI, R. (1998) Large Molecular Mass Materials in Coal-Derived Liquids by  $^{252}\text{Cf}$ -Plasma and Matrix-Assisted Laser Desorption Mass Spectrometry. *Energy & Fuels*, 12, 485-492.



- EDWARDS, I. A. S. (1989) Structure in Carbon and Carbon Forms. IN MARSH, H. (Ed.) *Introduction to Carbon Science*. Butterworth, Butterworth & Co.
- EDWARDS, W. F., JIN, L. & THIES, M. C. (2003) MALDI-TOF mass spectrometry: Obtaining reliable mass spectra for insoluble carbonaceous pitches. *Carbon*, 41, 2761-2768.
- EICHNER, T., BRAUN, M. & HÜTTINGER, K. J. (1996) Element-substituted polyaromatic mesophases: I. Boron-substitution with the pyridine-borane complex. *Carbon*, 34, 1367-1381.
- FIFIELD, F. W. & KEALEY, D. (1995) *Principles and Practice of Analytical Chemistry*, Great Britain, Chapman & Hall.
- FISCHER, P., STADELHOFER, J. W. & ZANDER, M. (1978) Structural investigation of coal-tar pitches and coal extracts by  $^{13}\text{C}$  n.m.r. spectroscopy. *Fuel*, 57, 345-352.
- FITZER, E., KÖCHLING, K.-H., BOEHM, H. P. & MARSH, H. (1995) Recommended Terminology for the Description of Carbon as a Solid. *Pure & Applied Chem*, 67, 473-506.
- FRACKOWIAK, E., MACHNIKOWSKI, J., KACZMARSKA, H. & BÉGUIN, F. (2001) Boronated mesophase pitch coke for lithium insertion. *Journal of Power Sources*, 97-98, 140-142.
- FRANKLIN, R. E. (1951) Crystallite Growth in Graphitizing and Non-Graphitising. *Proc. R. Soc.*, 209, 196-218.
- FU, H., ZOU, D., JIANG, Z., YANG, J., WANG, J. & XING, J. (2008) A study of Boron-Bearing Wear-Resistant Alloy Steel Liner. *Materials and Manufacturing Processes*, 23, 469-474.
- GARTON, F. W. J. (1957) The spectrographic determination of boron in graphite. *Spectrochimica Acta*, 9, 297-306.
- GAZI, M., GALLI, G. & BICAK, N. (2008) The rapid boron uptake by multi-hydroxyl functional hairy polymers. *Separation and Purification Technology*, 62, 484-488.
- GILLIN, L. M. (1967) Deformation Characteristics of Nuclear Grade Graphites. *Journal of Nuclear Materials*, 23, 280-288.
- GROSS, A., BERNSTEIN, A., VULKAN, R., TARCHITZKY, J., BEN-GAL, A. & YERMIYAHU, U. (2008) Simple digestion procedure followed by the

- azomethine-H method for accurate boron analysis and discrimination between its fractions in wastewater and soils *Chemosphere*, 72, 400-406.
- GUILLÉN, M. D., BLANCO, J., CANGA, J. S. & BLANCO, C. G. (1991) Study of Effectiveness of 27 Organic Solvents in the Extraction of Coal Tar Pitch. *Energy & Fuels* 5, 188-192.
- GUILLÉN, M. D., IGLESIAS, M. J., DOMÍNGUEZ, A. & BLANCO, C. G. (1992) Semiquantitative FTIR Analysis of Coal Tar Pitch and Its Extracts and Residues in Several Organic Solvents. *Energy & Fuels*, 6, 518-525.
- HALL, G., MARSDEN, B. J. & FOK, S. L. (2006) The microstructural modelling of nuclear grade graphite. *Journal of Nuclear Materials*, 353, 12-18.
- HAMADA, T., SUZUKI, K., KOHNO, T. & SUGIURA, T. (2002) Structure of coke powder heat-treated with boron. *Carbon*, 40, 1203-1210.
- HAUSLER, D. (1987) Trace element analysis of organic solutions using inductively coupled plasma-mass spectrometry. *Spectrochimica Acta*, 42B, 63-73.
- HAWTHORNE, M. F. (1991) Biochemical applications of boron cluster. *Pure & Applied Chem*, 63, 327-334.
- IEA (2006) World Energy Outlook. *World Energy Outlook*. Second ed. Paris Cedex, International Energy Agency.
- ISHII, T., ISHIBASHI, Y. & TAKEUCHI, C. (1984) Determination of Trace Amounts of Boron in Steel by Inductively Coupled Spectrometry Using Methyl Borate as Distillate. *Transaction ISIJ*, 24, 498-501.
- IWUNZE, M. O. (2004) Fluorescence Quenching Studies of Curcumin by Hydrogen Peroxide in Acetonitrile Solution *Monatshefte fur Chemie*, 135, 231-240.
- JEMMIS, E. D. & BALAKRISHNARAJAN, M. M. (2001) Polyhedral Boranes and Elemental Boron: Direct Structural Relations and Diverse Electronic Requirements. *J. Am. Chem. Soc.*, 123, 4324-4330.
- KELLY, B. T. (1981) Introduction Graphite. IN KELLY, B. T. (Ed.) *Physics of Graphite*. London and New Jersey, Applied Science Publishers.
- KIRK-OTHMER (2005) Graphite, Artificial. *Encyclopedia of Chemical Technology*. Wiley.

- LAVIN, J. G. (2001) Mesophase Precursors for Advanced Carbon Fibers IN RAND, B., APPELYARD, S. P. & YARDIM, M. F. (Eds.) *Design and Control of Structure of Advanced Carbon Materials for Enhanced Performance*. Netherlands, Kluwer Academic Publishers.
- LEVIN, M. & REDELIUS, P. (2008) Determination of Three-Dimensional Solubility Parameters and Solubility Spheres for Naphthenic Mineral Oils. *Energy & Fuels*.
- LEWIS, I. C. (1982) Chemistry of Carbonization. *Carbon*, 20, 519 - 529.
- LIM, Y. S. & LEE, B. I. (1991) Mesophase formation and chemical changes in petroleum pitch during low-temperature heat soaking. *Journal of Materials Science*, 26, 1039-1044.
- MARSH, H., MARTÍNEZ-ESCANDELL, M. & RODRÍGUEZ-REINOSO, F. (1999) Semicokes from pitch pyrolysis: mechanisms and kinetics. *Carbon*, 37, 363-390.
- MCHENRY, E. R. & SAVER, W. E. (1996) LABORATORY PITCH PAH AND POM STUDY. *TMS Annual Meeting*. Anaheim, California.
- MENÉNDEZ, R., BERMEJO, J. & FIGUEIRAS, A. (2000) Tar and Pitch: Composition and Application. IN MARSH, H. & RODRÍGUEZ-REINOSO, F. (Eds.) *Sciences of Carbon Materials*. Secretariado de Publicaciones.
- MOCHIDA, I., KORAI, Y., KU, C.-H., WATANABE, F. & SAKAI, Y. (2000) Chemistry of synthesis, preparation and application of aromatic-derived mesophase pitch. *Carbon*, 38, 305-328.
- MOCHIDA, I., KORAI, Y., WANG, Y.-G. & HONG, S.-H. (2001) Preparation and Properties of Mesophase Pitches. IN PIERRE, D. (Ed.) *Graphite and Precursors*. Gordon and Breach Science.
- MOKOENA, K., VAN DER WALT, T. J., MORGAN, T. J., HEROD, A. A. & KANDIYOTI, R. (2008a) Heat treatment of medium-temperature Sasol-Lurgi gasifier coal-tar pitch for polymerizing to higher value products. *Fuel*, 87, 751-760.
- MOKOENA, K., WALT, T. J. V. D., MORGAN, T. J., HEROD, A. A. & KANDIYOTI, R. (2008b) Heat treatment of medium-temperature Sasol-Lurgi gasifier coal-tar pitch for polymerizing to higher value products. *Fuel*, 87, 751-760.

- MONTES-MORÁN, M. A., CRESPO, J. L., YOUNG, R. J., GARCÍA, R. & MOINELO, S. R. (2002) Mesophase from a coal tar pitch: a Raman spectroscopy study. *Fuel Processing Technology*, 77-78, 207-212.
- MORIYAMA, R., HAYASHI, J.-I. & CHIBA, T. (2004) Effects of quinoline-insoluble particles on the elemental processes of mesophase sphere formation. *Carbon*, 42, 2443-2449.
- MORIYAMA, R., KUMAGAI, H., HAYASHI, J.-I., YAMAGUCHI, C., MONDORI, J., MATSUI, H. & CHIBA, T. (2000) Formation of mesophase spheres from a coal tar pitch upon heating and subsequent cooling observed by an in situ <sup>1</sup>H-NMR. *Carbon*, 38, 749-758.
- MUETTERTIES, E. L. (1967) General Introduction to Boron Chemistry. IN MUETTERTIES, E. L. (Ed.) *The chemistry of boron and its compounds*. New York, John Wiley & Sons Incl.
- MURTY, H. N., BIEDERMAN, D. L. & HEINTZ, E. A. (1977) Apparent catalysis of graphitisation.
3. Effect of boron. *Fuel*, 56, 305-312.
- NICHOLLS, D. R. (2000) Status of the pebble bed modular reactor. *Nuclear Energy*, 39, 231-236.
- OBERLIN, A. & BONNAMY, S. (2001) Carbonization and Graphitization. IN PIERRE, D. (Ed.) *Graphite and Precursors*. Gordon and Breach Science
- PASTO, D. J. & JOHNSON, C. R. (1989) *Laboratory Text for Organic Chemistry, A source for chemical and physical techniques*. , Englewood Cliffs, New Jersey, Prentice-Hall, Inc.,.
- PASZTOR, L., BODE, J. D. & FERNANDO, Q. (1960) Determination of Micro Quantities of Boron in Steel by a Solvent Extraction Method. *Analytical Chemistry*, 32, 277-281.
- PAYTON, F., SANDUSKY, P. & ALWORTH, W. L. (2007) NMR Study of the Solution Structure of Curcumin. *Journal of Natural Products*, 70, 143-146.
- PERKAMPUS, H.-H. (1992) *UV-VIS Spectroscopy and Its Application*, Dusseldorf, Springer-Verlag.

- PLEŠEK, J. (1992) Potential Applications of Boron Cluster Compounds. *Chem. Rev.*, 92, 269-278.
- RAMANJANEYULU, P. S., SAYI, Y. S. & RAMAKUMAR, K. L. (2008) Determination of boron in uranium-aluminum-silicon alloy by spectrophotometry and estimation of expanded uncertainty in measurement. *Journal of Nuclear Material*, 378, 139-143.
- RAND, B. (2001) The Thermal Processing and Rheological Behaviour of Pitch IN RAND, B. (Ed.) *Design and Control of Structure Advanced Carbon Materials for Enhanced Performance*. Netherlands, Kluwer Academic Publishers
- RAND, B., HOSTY, A. J. & WEST, S. (1989) Physical Properties of Pitch Relevant to the Fabrication of Carbon Materials. IN MARSH, H. (Ed.) *Introduction to Carbon Science*. London, Butterworths & Co.
- RAND, B., WESTWOOD, A. V. K. & LU, S. (2001) Carbon-ceramic alloys. IN RAND, B., APPELYARD, S. P. & YARDIM, M. F. (Eds.) *Design and Control of Structure of Advanced Carbon Materials for Enhanced Performance*. Netherlands, Kluwer Academic Publishers.
- RAO, R. M. & AGGARWAL, S. K. (2008) Determination of boron at sub-ppm levels in uranium oxide and aluminum by hyphenated system of complex formation reaction and high-performance liquid chromatography (HPLC). *Talanta*, 75, 585-588.
- SAH, R. N. & BROWN, P. H. (1997) Boron Determination-A Review of Analytical Methods. *MICROCHEMICAL JOURNAL*, 56, 285-304.
- SIMA, L., BLANCO, C., SANTAMARIA, R., GRANDA, M., SLAGHUIS, H. & MENENDEZ, R. (2003) Relationship between chemical composition and pyrolysis behaviour of a medium temperature pitch. *Fuel Processing Technology*, 84, 63 - 77.
- SINGER, L. S., LEWIS, I. C., RIFFLE, D. M. & DOETSCHMAN, D. C. (1987) EPR Characteristics of Separated Fractions of Mesophase Pitches. *The Journal of Physical Chemistry*, 91, 2408-2415.

- STEFANOVA, M., MARINOV, S. P. & LAZOROV, L. (1995) Thermochemical transformation of the quinoline-soluble portion of coal tar pitch. *Fuel*, 74, 990-994.
- THANGAVEL, S., DHAVILE, S. M., DASH, K. & CHAURISA, S. C. (2004) Spectrophotometric determination of boron in complex matrices by isothermal distillation of borate ester into curcumin. *Analytica Chimica Acta* 502, 265-270.
- THANGAVEL, S., RAO, S. V., DASH, K. & ARUNACHALAM, J. (2006) Determination of boron isotope ratios by Zeeman effect background correction-graphite furnace atomic absorption spectrometry. *Spectrochimica Acta Part B* 61, 314 - 318.
- UPPSTRÖM, L. R. (1968) A modified method for determination of boron with curcumin and a simplified water elimination procedure. *Analytica Chimica Acta*, 43, 475-486.
- WANG, X. M. & HE, X. L. (2002) Effect of Boron Addition on Structure and Properties of Low Carbon Bainitic Steels. *ISIJ International*, 42, S38-S46.
- WATSON, J. T. & SPARKMAN, O. D. (2007) *Introduction to mass spectrometry: instrumentation, applications and strategies for data interpretation*, Chichester, John Wiley & Sons.
- WILLIAMS, L. B., HERVIG, R. L., WIESER, M. E. & HUTCHEON, I. (2001) The influence of organic matter on the boron isotope geochemistry of the gulf coast sedimentary basin, USA. *Chemical Geology*, 174, 445-461.
- WOODS, W. G. (1994) An Introduction to Boron: History, Sources, Uses, and Chemistry. *Environmental Health and Perspectives*, 102, 5-11.
- XU, Y. & JIANG, J.-Q. (2008) Technologies for Boron Removal. *Ind. Eng. Chem. Res.*, 47, 16-24.
- YAMANE, T., KOUZAKA, Y. & HIRAKAWA, M. (2001) Continuous flow system for the determination of trace boron in iron and steel utilizing in-line preconcentration/separation by Sephadex column coupled with fluorimetric detection. *Talanta*, 55, 387-393.
- YARDIM, M. F. & EKINCI, E. (2001) Pitch precursor-origin and chemical constitution. IN RAND, B., APPELYARD, S. P. & YARDIM, M. F. (Eds.) *Design and*

- Control of Structure of Advanced Carbon Materials for Enhanced Performance.*  
Netherlands, Kluwer Academic Publishers.
- YARDIM, M. F., EKINCI, E. & BARTLE, K. D. (2001) Pitch precursor-origin and chemical constitution. IN RAND, B., APPELYARD, S. P. & YARDIM, M. F. (Eds.) *Design and Control of Structure of Advanced Carbon Materials for Enhanced Performance.* Netherlands, Kluwer Academic Publishers.
- YOON, K. J. & KIM, K.-J. (1985) Double Ion-Pair Formation in Aqueous Solutions of Methylene Blue and Tetraphenylborate. *Bull. Korean Chem. Soc.*, 6, 149-152.
- YURIOKA, N. (2001) Physical Metallurgy of Steel Weldability. *ISIJ International*, 41, 566.
- ZANDER, M. (2000) Chemistry and Properties of Coal-Tar and Petroleum Pitch. IN MARSH, H. & RODRÍGUEZ-REINOSO, F. (Eds.) *Sciences of Carbon Materials.* Secretariado de Publicaciones.